Tectonophysics 474 (2009) 367–392

Contents lists available at ScienceDirect

Tectonophysics

journal homepage: www.elsevier.com/locate/tecto

From outcrop and petrographic studies to basin-scale fluid flow modelling: The use of the Albanian natural laboratory for carbonate reservoir characterisation

Nadège Vilasi [a,b,*], Julien Malandain [a,c], Laurie Barrier [d], Jean-Paul Callot [a], Khalid Amrouch [a,c], Nicole Guilhaumou [e], Olivier Lacombe [c], Kristaq Muska [f,g], François Roure [a,h], Rudy Swennen [b]

[a] Direction Géologie–Géochimie–Géophysique, IFP, 1-4 Avenue de Bois-Préau, F-92852 Rueil-Malmaison Cedex, France
[b] Geo-Institute, Dept. of Earth and Environmental Sciences, KU-Leuven, Celestijnenlaan 200E, B-3001 Leuven, Belgium
[c] Université Pierre et Marie Curie-Paris 6, Laboratoire de Tectonique, UMR 7072 CNRS, Aile 46-45, 2° étage, 4 Place Jussieu, F-75252 Paris Cedex 05, France
[d] Laboratoire de Tectonique Continentale, Tour 14-24, 1° étage, Aile 14-24, IPGP, Institut de Physique du Globe de Paris, 4 Place Jussieu, 75252 Paris Cedex 05, France
[e] MNHN, Museum National d'Histoire Naturelle, Laboratoire d'étude de la matière extra-terrestre, 57 rue Cuvier, F-75005 Paris, France
[f] Geology Department, Polytechnic Institute, University of Tirana, Albania
[g] National Scientific Center of Hydrocarbon, Fier, Albania
[h] Vrije Universiteit Amsterdam, Netherlands

ARTICLE INFO

Article history:
Received 14 February 2008
Received in revised form 5 January 2009
Accepted 26 January 2009
Available online 14 February 2009

Keywords:
Foreland fold-and-thrust belt
Geochemistry
Paleofluids
Calcite twins
Diagenesis
Carbonate reservoirs
Fluid flow
Migration pathways
Kinematic modelling
Fault permeability
Hydrocarbon migration
Heat flow

ABSTRACT

The Albanian fold-and-thrust belt and the Peri-Adriatic Depression are well documented by means of seismic reflection profiles, GPS reference points, potential data, wells and outcrops. The continuous Oligocene to Plio-Quaternary sedimentary records help to constrain both the burial history of Mesozoic carbonate reservoirs, the timing of their deformation, and the coupled fluid flow and diagenetic scenarios.

Since the mid-90s, the Albanian foothills were used as a natural laboratory to develop a new integrated methodology and work flow for the study of sub-thrust reservoir evolution, and to validate on real case studies the use of basin modelling tools as well as the application of new analytical methods for the study petroleum systems in tectonically complex areas.

The integration of the interactions between petrographic and microtectonic studies, kinematic, thermal and fluid flow basin modelling, is described in detail. The fracturing of the reservoir intervals has a pre-folding origin in the Albanides and relates to the regional flexuring in the foreland. The first recorded cement has a meteoric origin, implying downward migration and the development of an earlier forebulge in the Ionian Basin. This fluid, which precipitates at a maximum depth of 1.5 km, is highly enriched in strontium, attesting for important fluid–rock interaction with the Triassic evaporites, located in diapirs. From this stage, the horizontal tectonic compression increases and the majority of the fluid migrated under high pressure, characterised by brecciated and crack-seal vein. The tectonic burial increased due to the overthrusting, that is pointed out by the increase of the precipitation temperature of the cements. Afterwards, up- or downward migration of SO_4^{2-}, Ba^{2+} and Mg^{2+}-rich fluids, which migrated probably along the décollement level, allows a precipitation in thermal disequilibrium. This period corresponds to the onset of the thrusting in the Ionian Zone. The last stage characterised the uplift of the Berati belt, developing a selective karstification due likely to the circulation of meteoric fluid.

The main results of the fluid flow modelling show that the Upper Cretaceous–Paleocene carbonate reservoirs in the Ionian zone have been charged from the Tortonian onward, and that meteoric fluid migration should have intensely biodegraded the hydrocarbon in place. Concerning the migration paths, it has been demonstrated that the thrusts act principally as flow barriers in Albania, mainly due the occurrence of evaporites (non-permeable), except in the foreland, where they do not occur.

1. Introduction

The main challenge for the study of sedimentary basins relates to the coupling and interactions between various processes, acting either deep in the lithosphere and crust (i.e., the heat flow and tectonic subsidence), at shallower burial levels in the sediments (i.e., the diagenesis), or eventually at the surface (i.e., erosion and sedimentation), in the course of ongoing deformation. The more we learn on sedimentary basins, the more we identify the need for integration of data and expertise from various disciplines such as (1) geophysics, structural geology and sedimentology to properly describe at different scales the architecture, dynamic and sedimentary infill of the basin,

* Corresponding author. Direction Géologie–Géochimie–Géophysique, IFP, 1-4 Avenue de Bois-Préau, F-92852 Rueil-Malmaison Cedex, France.
E-mail address: nvilasi@yahoo.fr (N. Vilasi).

0040-1951/$ – see front matter © 2009 Elsevier B.V. All rights reserved.
doi:10.1016/j.tecto.2009.01.033

but also (2) petrography, geochemistry and basin modelling, that are ultimately required to reconstruct the evolution of the porous medium through time and to provide realistic predictions (quantification) of present-day characteristics of the reservoirs in areas that have not yet been investigated by drilling.

From 1996 to 2002, collaborative studies dedicated to the prediction of reservoir characteristics, coupling both petrographic work and basin modelling, have been the driving force of the SUB-Thrust Reservoir APpraisal joint industry project (SUBTRAP Consortium; Roure et al., 2005), with case studies dedicated to sandstone reservoirs in Sub-Andean Basins in Venezuela and Colombia, and to carbonate reservoirs in Pakistan, Mexico, Canada, as well as in Albania (Swennen et al., 1999; Ferket et al., 2000; Swennen et al., 2000; Van Geet et al., 2002; Benchilla et al., 2003; Ferket et al., 2003; Vandeginste et al., 2005; Breesch et al., 2006; Ferket et al., 2006; Breesch et al., 2007; Vandeginste et al., 2006; Vilasi et al., 2006; Dewever et al., 2007).

During the Albanian part of the SUBTRAP project and subsequent collaborations with the Albanian Petroleum Institute in Fier, Triassic dolomites (Muska, 2002) and Upper Cretaceous carbonate turbidites (Swennen et al., 2000; Van Geet et al., 2002; Dewever et al., 2007) have been successively studied. We have also extended the quantification to kinematic and sedimentary modelling by coupling Thrustpack with Dionisos (Barrier et al., 2003, 2005), as well as to fluid flow, pore fluid pressure and hydrocarbon migration modelling with Ceres (this study). Other projects supported by NATO (Science for Peace Programme) have also provided new information on tectonically active features of the Albanian foothills (synthesis on current seismicity, focal mechanisms and GPS measurements; Nieuwland et al., 2001; Kiratzi and Muço, 2004), as well as on the timing of tectonic uplift and unroofing of the hinterland (Apatite Fission Tracks; Muceku, 2006; Muceku et al., 2006), making Albania one of the best documented natural laboratory for the study of active European onshore compressional systems.

2. Architecture, evolution and data base of the Albanian natural laboratory

2.1. Geological and geodynamical background of the Albanian foothills and Peri-Adriatic Depression

The Albanian foothills result from the Neogene deformation of the former eastern passive margin of Apulia. Located west of the Mirdita ophiolite and the Kruja Zone (Fig. 1A), the outer zones of the Albanian thrust belt are subdivided in two very distinct tectonic provinces by the NE-trending Vlora-Elbasan lineament, with up to 10 km of Oligocene to Plio–Quaternary clastics being still currently preserved in the Peri-Adriatic Depression in the north, and Mesozoic carbonates of the Ionian Zone being directly exposed at the surface in the south (Fig. 1A and C). As evidenced on seismic profiles, the main décollement level is localised within Triassic evaporites and salt in the south, ramp anticlines accounting for the tectonic uplift of Mesozoic carbonates in the Ionian Zone, whereas it is located within the Cenozoic clastics in the north, where no carbonate reservoirs are exposed at the surface. Accordingly, the Vlora-Elbasan transfer zone is best described as a lateral ramp connecting these two distinct décollement surfaces (Roure et al., 1995). The tectono-stratigraphic evolution of the outer Albanides can be summarised as follows (Fig. 1B).

2.1.1. Evolution of the Tethyan passive margin and deposition of carbonate reservoirs

Tethyan rifting accounts for the development of Late Triassic to Liassic tilted blocks and grabens, thick organic-rich dolomitic platform carbonates characterising the paleo-horsts, whereas Liassic blackshales (Posidonia shale) were deposited in the grabens (Meço and Aliaj, 2000; Zappatera, 1994), thus accounting for the two main source rocks intervals of the basin. Post-rift thermal subsidence resulted in the deposition of deep water cherts during the Middle and Upper Jurassic in the Ionian Basin, whereas prograding Cretaceous carbonate platforms from the Kruja Zone in the east, and from the Sazani Zone in the west, contributed as a distal source for the thick carbonate turbidites deposited in the Ionian Basin during the Late Cretaceous and Paleocene (Velaj et al., 1999). These turbidites, which reworked platform carbonate material (Van Geet et al., 2002), are interbedded within finer grained pelagic carbonates, and constitute the main hydrocarbon reservoirs onshore Albania, but also offshore in the Italian part of the Adriatic Sea.

2.1.2. Foothills development and sedimentary records of the deformation

Up to 10 km of synflexural and synkinematic siliciclastic series have been deposited in the Peri-Adriatic Depression, ranging from near-shore and littoral facies in the east and south, toward deeper water and turbiditic facies in the north and in the west (offshore), providing a unique and continuous sedimentary record of the deformation (Frasheri et al., 1996). Sequence stratigraphy and biostratigraphy by means of foraminifer and nannoplancton in pelagic facies are able to provide accurate correlations of very good resolution for the dating of geologic events in this basin:

(1) Tectonic loading applied by the hinterland (Mirdita ophiolite) from the Upper Cretaceous onward and westward thrusting of far travelled basinal units of the Krasta Zone induced the progressive development of a wide flexural basin, which ultimately impacted the outer Albanides lithosphere in Oligocene times (Shallo, 1991; Kodra and Bushati, 1991; Melo et al., 1991a,b; Shallo, 1992).
(2) Growth anticlines started to develop in Late Oligocene–Aquitanian in the Ionian Basin (Velaj et al., 1999; Meço and Aliaj, 2000; Robertson and Shallo, 2000; Nieuwland et al., 2001), accounting for the development of Burdigalian reefal facies and paleo-karst at the crest of the Kremenara anticline, this main episode of shortening being sealed by Langhian–Serravalian clastics (Van Geet et al., 2002).

The second episode of tectonic shortening is best documented near the Vlora-Elbasan transfer zone (Roure et al., 1995) and farther north in the Peri-Adriatic Depression, where Pliocene backthrusts account for major lateral and vertical offsets of a pre-Messinian erosional surface. Although Neogene deposits are mostly absent from the Ionian Zone itself, it is obvious that this post-Messinian tectonic episode strongly affected also the southern part of the Albanian Foothills, thus increasing the deformation in both Kremenara and Saranda anticlines, which will be discussed in more detail below (Tagari, 1993).

Apart of thrusting and development of ramp anticlines, these Neogene episodes of deformation have also contributed to remobilise former salt diapirs, i.e. in the Dümre area (Fig. 1A; Monopolis and Bruneton, 1982; Underhill, 1988; Bakiaj and Bega, 1992; Velaj and Xhufi, 1995), where an allochthonous salt unit has been thrusted along a low angle fault over underlying carbonate duplexes and deformed Cenozoic clastics. At this stage, however, it is difficult to date the onset of the salt motion, and at which time Triassic salt indeed breached the surface (Velaj et al., 1999). High Sr-contents of some paleofluids with otherwise meteoric signature may account for early exposures of the Triassic salt (Travé et al., 2000), and one of the current challenge is to determine whether this exposure pre-dates or post-dates the onset of thrusting.

2.2. Ongoing integrated work

Coupling kinematic, thermal and petroleum Thrustpack modelling has already been attempted along various transects of the outer Albanides, where the database and paleothermometers (Ro, *T*max) are plenty, in order to account for the timing of the hydrocarbon generation in both the Ionian Basin and underthrust units, which are currently buried beneath the Kruja Zone (Roure et al., 2004). Basin modelling results, presented below, refer to additional coupling made with Thrustpack and Dionisos in order to better predict the spatial and

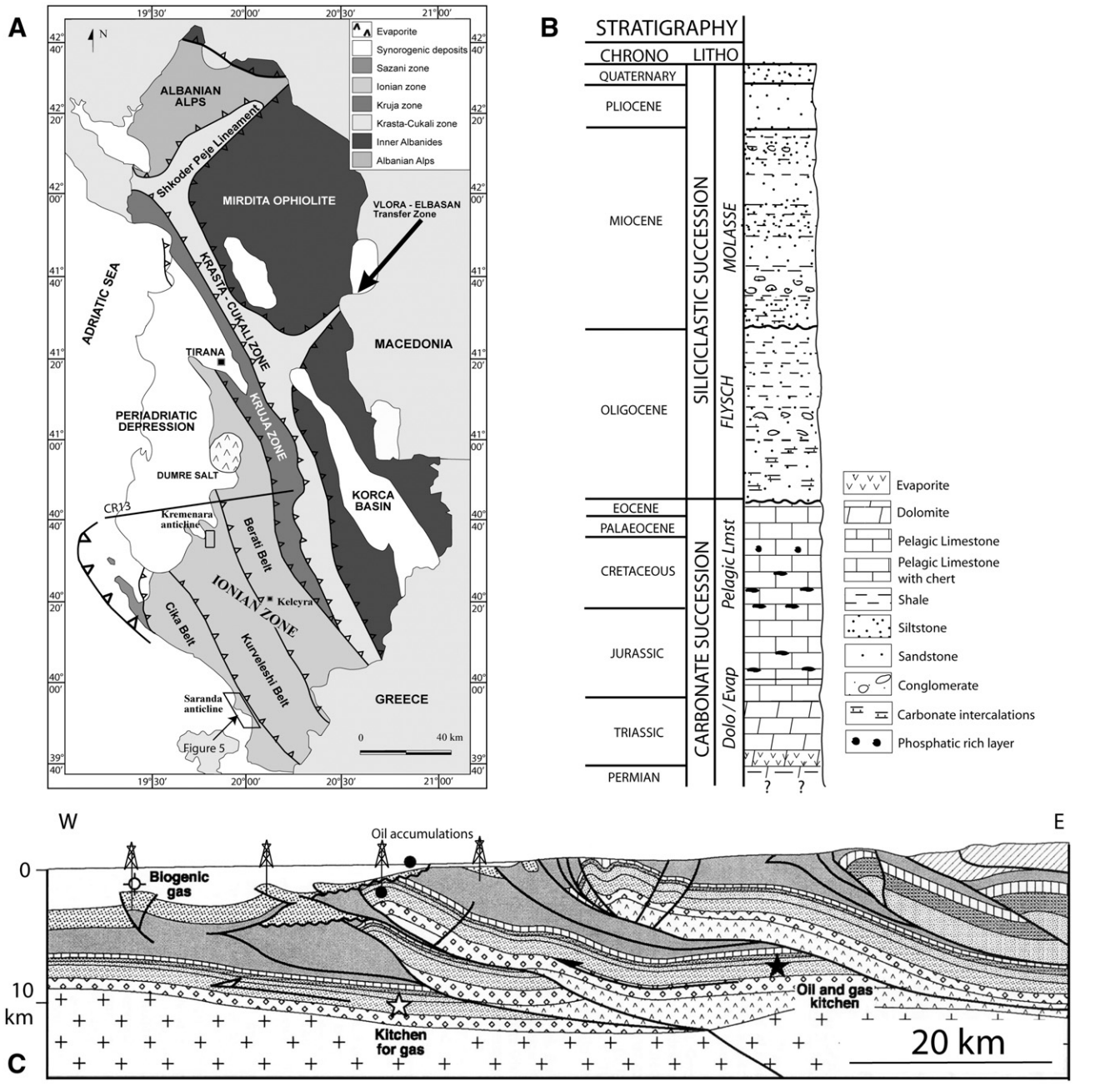

Fig. 1. (A) Structural map of the Albanides with location of the studied areas (e.g. Kelcyra quarry, Kremenara and Saranda anticlines). CR13 line represents the geological profile (C), interpreted from seismic lines crossing the outer Albanides (from Roure et al., 2004). (B) Representative stratigraphic section for the Ionian Zone (Kurveleshi unit). The location of Fig. 5 is shown on the structural map (A). Vertical scale is approximate as exact thicknesses are unknown (Van Geet et al., 2002).

temporal distribution of clastic reservoirs (Barrier et al., 2003, 2005), and to Ceres fluid flow and pore fluid pressure reconstructions, aiming at a better coupling between deformational pore-fluid pressure and fluid flow appraisal of carbonate reservoirs.

New apatite fission tracks and (U–Th)/He thermochronology from the Mirdita allochthon (Muceku, 2006; Muceku et al., 2006) have provided new evidence for the early unroofing of the hinterland, which predates the thrust emplacement of the allochthon over the outer Albanides. The western Internal Albanides is characterised by slow cooling and low exhumation rate (<0.1 km/my) throughout the Late Eocene that are related to isostatic uplift as a consequence of crustal thickening near the frontal thrust. At present-day, Muceku (2006) demonstrates that the symmetric structure of the ophiolite units in the Internal Albanides is a result of Mio–Pliocene extensional collapse, affecting the eastern ophiolites and the Korabi Zone. Apart of providing new challenges for Topo-Europe (Cloetingh and Topo-Europe team, 2005), these new paleo-topographic constraints may open new perspectives for the exploration of sub-thrust units located east of the Kruja front, as they may have escaped cracking beneath a thinner-than-expected allochthon. Proper risk appraisal would however still require to perform a complete coupled kinematic and thermal modelling across the Inner Albanides, using these new data, in order to reconstruct the complete burial and maturation history of potential source rocks in the underthrust foreland.

3. Paragenetic sequence in Late Cretaceous–Early Tertiary reservoirs and characterisation of paleofluid flow

In an attempt to deduce the main processes controlling the diagenetic evolution of the main reservoirs as well as to reconstruct

the fluid flow history in the foreland thrust system, several studies have been carried out on: (1) the role of the Upper Triassic evaporites (Swennen et al., 1999; Muska, 2002; De Paola et al., 2007), (2) the dual (matrix and fracture) porosity evolution of the Upper Cretaceous to Eocene carbonates (Swennen et al., 2000; Van Geet et al., 2002; Dewever et al., 2007), and (3) the reconstruction of the entire fluid rock interaction history through time and space (this study). The combination of these previous studies in conjunction with our new results allows to establish a precise paragenetic sequence. Major attention will be paid to characterise the timing of the overpressures that relate to tectonic deformation. The section below focuses on the Triassic and Cretaceous to Eocene carbonates only. The intervening Jurassic to Lower Cretaceous series have not been studied since they consist of deep marine non porous carbonates.

3.1. Triassic dolomites and evaporites

Since many years, the Palaeozoic and Permian–Triassic platform carbonates associated with evaporites have been of major interest for petroleum exploration in the Mediterranean region (e.g. Italy, Spain, Greece; Travé et al., 2000; Marfil et al., 2005). The interplay between carbonates and evaporites is very significant during any orogenic activity, as it controls the seal characteristics of the reservoirs, their ductile behaviour during tectonic deformation, the occurrence of high thermal conductivities, and diagenetic processes (i.e. tectonic-induced dolomitisation). Sometimes the potential reservoir qualities of carbonates can improve, especially in relation to the dehydration of the gypsum that can create overpressured regimes and consequently hydrofracturing (De Paola et al., 2007) during the burial stage. At present, the Upper Triassic dolomitic interval consists of cyclic sequences, characterised by occurrence of mud at the base, followed by evaporitic strata, containing many chicken wire fabrics, and dolomite collapse breccias at the top, testifying of the dissolution of the evaporites.

In the Ionian Zone, the Triassic evaporitic succession (i.e. an alternation of gypsum-anhydrites, dolostones and clays) is locally up to 2.5 km thick. The latter reflects hypersaline, shallow-water depositional conditions.

3.1.1. Evaporitic occurrences

Lower Triassic evaporites (i.e. mainly gypsum) are widespread in the Albanides and constitute the main décollement level of the Albanides Foreland Fold-and-Thrust Belt (FFTB). Triassic evaporites locally crop out but are more common in the subsurface, where they either form diapirs or flow along main faults. Two main types of diapirs (Velaj, 2001) are recognised in the Ionian Basin: (a) those that are emplaced along longitudinal tectonic faults (i.e. NNW–SSE thrusting faults), where they intersect transversal ones (i.e. NE–SW rifting faults), as the Dümre diapir (Fig. 1A); and (B) diapirs that are located in local structures such as in the core of anticlines (i.e. the Delvina, Bashaj, Fterra diapirs).

Since the mechanical properties of the evaporites changed through the geodynamic evolution of the basin, according to the applied stress, pressure and temperature regimes, the mode of formation of diapirs is actually still discussed. After sedimentation the first step of their formation occurred prior to the orogeny during the extension stage (i.e. rifting period) from the Upper Triassic till the Lower Cretaceous. During this period, the light evaporites have migrated vertically according to the gravitational forces. They have been subsequently affected from the Oligocene onward by folding and thrust tectonics. The normal faults were then reactivated and inverted as thrusts or strike–slip faults, forcing the evaporites to move towards lower pressure gradients. According to Velaj (2001), most Albanian diapirs have been thrusted westward with a displacement exceeding 20–30 km, which is in agreement with the average shortening of the main thrust units.

3.1.2. Dolomitic intervals

Recently, Triassic evaporitic, shaly and dolomitic intervals, cropping out in the south-western part of the Ionian Basin (Kurveleshi unit, Delvina area) have been investigated by Muska (2002), especially in an attempt at understanding the formation of the Upper Triassic dolomites and the thermal evolution of the Kurveleshi tectonic unit. It appears, based on diagenetic and kinematic modelling studies, that the dolomites are not precursor and come from the early dolomitisation of the initial carbonated matrix, deposited during the rifting stage. This diagenetic process occurred afterwards the dissolution and the brecciation of the Triassic evaporites during the burial phase. The fluid inclusion analyses, performed on these dolomites, display a maximum homogenisation temperature of 80 °C (Muska, 2002), which can be related to the maximum burial during the Late Oligocene. However, the thermal evolution of the Triassic interval is not homogeneous along the Albanides, since the tectonic units have not been formed and thrusted simultaneously. In fact, the Kurveleshi unit was the first unit to be uplifted with the Cika belt, whereas the Berati and Kruja units have been formed out-of-sequence (Fig. 10). Finally, even if only low temperature dolomites occur in the Delvina oil field (in Kurveleshi unit), high temperature dolomites may exist locally in deeper buried structures (i.e. Berati and Kruja units).

In order to trace a possible interaction of Triassic evaporites with fluids, the Triassic evaporates–dolomites, located in the south Albania, i.e. Mali Gjere section, have been isotopically characterised in the framework of the SUBTRAP consortium (Swennen et al., 1999). The evaporitic interval displays a Sr^{87}/Sr^{86} of 0.707777 ($^{+}/-0.000020$), whereas the dolomitic layers have higher values of 0.708010 and 0.709498 ($^{+}/-0.00003$). The carbon and the oxygen values of the dolomite/evaporite section plot respectively from −3 to +0.9‰ V-PDB and from −0.7 to −2.15‰ V-PDB. The section, where only dolomites occur, possess $\delta^{13}C$ between −0.7 and 0.9‰ V-PDB and $\delta^{18}O$ from −0.35 to −2.75‰ V-PDB.

3.2. Dual matrix–fracture porosity of Upper Cretaceous to Eocene limestone reservoirs

The study of the matrix porosity represents a major interest for carbonate reservoir characterisation, since active tectonic deformation can generate a succession of diagenetic processes due to important fluid migrations. Determining the evolution of the porosity is a complicated task and requires good and precise sampling and petrography. The fractured Upper Cretaceous to Paleocene carbonate turbidites of the Ionian Basin, which are made up of classical turbidites or Bouma sequences (Bouma, 1962), constitute an excellent rock-type to study the dual matrix and fracture porosity characteristics and thus the reservoir evolution.

3.2.1. Matrix porosity of carbonate turbidites

Exposed Cretaceous to Eocene limestone turbidites constitute reservoir analogues for the deep water carbonate reservoir interval of the Mediterranean zone (Albpetrol, 1993). They are equivalent to the Scaglia carbonate formation in Italy (Cazzola and Soudet, 1993), and have been studied in the Kremenara anticline (northern part of the Ionian Zone), which has the specificity to reveal oil seeps in a dual matrix–fracture porosity.

Carbonate turbidites of the Ionian Zone display important matrix deformation due to the successive diagenetic processes. Van Geet et al. (2002) and Dewever et al. (2007) described precisely these lithological intervals and the different diagenetic processes controlling the matrix porosity evolution (i.e. creation and/or destruction).

Petrography and porosity measurements demonstrate that the actual porosity and permeability distributions are principally controlled by initial sedimentological contrasts (fabric, mineralogy) and the eogenetic dissolution/precipitation, which occurred since the onset of the burial history. Turbidite beds, which are thicker than

Table 1
Summary of the petrographic, cathodoluminescence, geochemical, isotopic data and fluid inclusion for calcite and dolomite cements.

Cements	Frac. generation	Petrographic characteristics			Geochemical characteristics					Th (°C)	Salinity (wt.% NaCl)
		Optical microscope	CL	Other minerals	$\delta^{18}O$–$\delta^{13}C$ (‰)	Sr^{87}/Sr^{86}	Sr (ppm)	Mg (ppm)	Fe (ppm)		
Cal-2	N150°, 80S	Blocky calcite	Minor sector-zoning, from dull to bright CL	Strontianite, quartz and barite	$\delta^{13}C = +1.18$ to -6.32 $\delta^{18}O = -3.98$ to -2.82	0.707770	3678	1010	523	<40–50	21.9 to 35
		Non transparent, large and blocky calcite crystals	Light sector zoning from dull to orange CL, Partially recrystallised	Dol-1 (10%), barite, celestite and strontianite	$\delta^{13}C = -1.68$ to -3.00 $\delta^{18}O = -2.10$ to $+0.10$		2238	3263	<dl	95 to 142 (Recrystallisation)	0 to 8.4
Cal-3	N138°, 83S N150°, 80S	Non transparent, large and blocky elongated calcite crystals	Recrystallised	Dol-1 (10%)	$\delta^{13}C = +0.56$ to $+1.92$ $\delta^{18}O = -2.52$ to -0.40	0.707823	653	2775	185	34 to 60 Recrystallisation or heterogenous entrapment	19 to 30
		Blocky to elongated	Recrystallised	Dol-2, barite, Fe-oxides, strontianite and quartz	$\delta^{13}C = 0.67$ to 1.74 $\delta^{18}O = -0.13$ to $+1.66$		623	2237	<dl	120 to 140 (Recrystallisation?)	14 to 24.4
Cal-4	Parallel to BPS	Fibrous to elongated calcite crystals	Dull	Pyrite and barite	$\delta^{13}C = 1.61$ $\delta^{18}O = -5.57$		597	440	597		
Cal-5	N138°, 83S	Elongated to blocky calcite crystals with regularly spaced trails of pieces of wall rocks	Dull	Pyrite, quartz and barite, Dol-2	$\delta^{13}C = 1.28$ to 1.92 $\delta^{18}O = -5.78$ to -1.48		3573	1550	2193		
Cal-6	–	Blocky	Dull	Pyrite and quartz	$\delta^{13}C = 0.82$ $\delta^{18}O = -2.88$		255	2425	<dl		
Cal-7	N138°, 83S N03°, subvertical	Blocky	Dull sector zoned	Fluorite, Feldspath, Dol-2 (partially calcitised)	$\delta^{13}C = 1.91$ to 2.09 $\delta^{18}O = 0.12$ to 1.12	0.708039	54	3466	<dl		
Cements	Fracture	Optical microscope	CL	Other minerals	$\delta^{18}O$–$\delta^{13}C$ (‰)	Fe (ppm)	Sr (ppm)	Si (ppm)	Mn (ppm)		
Dol-1	–	Micrometric sub- to euhedral crystals	Red-dull	Strontianite (4%), Barite	$\delta^{13}C = 0.82$ to 0.94	11700	2963	<dl	1300		
Dol-2	N138°, 83S N150°, 80S	Non-transparent rhombohedric crystals	Red-dull partially calcitised (bright CL)	Phyllosilicates, Quartz, Barite	$\delta^{18}O = -1.75$ to -0.9 Dol-2 predominantly (dolomite correction)	1243	822	450	472		
Dol-3	N138°, 83S	Coarse subhedral and transparent crystals; exhibit slighlty curved surfaces	Red-dull	Barite	$\delta^{13}C = 0.26$ $\delta^{18}O = -12.21$ (dolomite correction)	<dl	<dl	200	375		

The abundance of various chemical elements was analysed by using electron microprobe.

35 cm, i.e. B to C horizons of the Bouma sequences, still possess some primary matrix porosity over one third of the bed thickness. The occurrence of diagenetic processes such as dissolution, cementation, neomorphism and compaction, operating shortly after the deposition, modified the primary porosity characteristics and distribution. Today, the matrix porosity is only preserved in the bioclastic grain- to packstones (i.e. middle part of the turbidite beds), where syntaxial cementation around rudist and crinoid fragments (i.e. ideal substrates for calcite cementation) stabilised the framework (Dewever et al., 2007; Swennen et al., 2000). Here, the dissolution of aragonite components plays a major role in the reservoir characteristics. Its dissolution increases the matrix porosity and saturates the expulsed fluid in HCO_3^- and Ca^{2+}, thus allowing to stabilise the pore network by inducing a rapid cementation, wherever nucleation sites occurred (Halley et al., 1984; Hendry et al., 1996). However, when no substrate for cementation occurs, the porosity is lost by compaction. This is the case for the A and D horizons, which are characterised by high matrix micrite content. Consequently, even if the lithology displays good initial porosity, the reservoir characteristics evolve drastically according to the diagenetic events like aragonite dissolution, burial compaction, and stabilisation of the pore network.

3.2.2. Fracture and stylolite porosities as a function of tectonic stresses

During the Albanides FFTB development, the carbonates of the Ionian Zone have been subjected to several stylolitisation processes and fracturing events, being subsequently filled by various calcite cements. In the case of Kremenara anticline and in some other locations in the vicinity of transfer zones, many fractures and stylolites are impregnated by oil due to a late reactivation of the structures (Roure et al., 2004).

During field campaigns, structural characterisation of stylolites, fractures was realised in three reservoir analogues (e.g. Kremenara and Saranda anticlines, Kelcyra outcrop), based principally on cross-cutting relationships between fractures and stylolites, unfolded orientations (i.e. azimuth and dip) and density measurements.

Two episodes of development of burial stylolites and of tectonic stylolites, related to the kinematic evolution of the FFTB, have been identified. The first generation of burial stylolitic planes forms mainly parallel to the depositional fabric (i.e. bedding). They formed during the burial stage before thrusting, which should consider to be Lower to Middle Oligocene. The second recorded BPS, which crosscuts the first one, was determined in the Kremenara anticline and is dated as post-folding. It must be related to a second post-Miocene burial phase (Breesch et al., 2007).

The tectonic stylolites record two dominant directions of the main principal stress σ1, respectively trending about N70°, which is roughly orthogonal to the frontal thrusts, and N160° (after rotation according to the bedding). However some uncertainties still exist concerning the chronology between both phases of tectonic stylolite development, since no cross-cutting relationship has been observed.

The N70° oriented σ1 is consistent with the main compression developing the NNW–SSE thrusts and folding structures in the Albanides. Tectonic stylolites should record a syn- to post-deformational stage, since they are roughly orthogonal to the direction of maximum stress and mostly parallel to the fold axes.

The second recorded maximum stress shows either a pre-folding NNW–SSE compression or a post-folding NW–SE compression. This change in the orientation of the maximum stress attests of the occurrence of a second main tectonic phase.

This deformation stage is also characterised by five generations of fractures. The first main orientation characterises the pre-folding stage and trends about N150° with subvertical dip (see Table 1, Cal-2). The second generation is oriented N138° with subvertical dip and interpreted as pre-folding. These fractures represent the most important fracturing stage during the Albanides FFTB development. Both fracture generations developed simultaneously with the regional flexuring of the foreland and could be contemporary with the maximum burial in the basin, under high fluid pressure (see also discussion on calcite twins in Section 4, set I veins).

Subsequently, other generations of fractures developed, the later being only observed in the anticlines of Kremenara and Saranda. These younger fractures characterise the evolution of the folding stage in the Ionian fronts. The first fractures are sub-parallel to the bedding and characterise the syn-folding displacement along bed contacts. The second stage is defined by a main N60° orientation of fractures with subvertical dip angle, which is consistent with the main compressional stress in the Albanides (i.e. Section 4, set II). It may be linked with the syn-folding stage. The last main fracturing stage is still syn-folding and trends about N110° with subvertical dip. This conceptual model is in agreement with the work published by Graham-Wall et al. (2006).

A last generation defined by N–S orientation (Table 1; Cal-7) with subvertical dip has also been observed but unfortunately without relationship with stylolites. Assuming a syn- or post-deformational origin, these fractures may be linked to an E–W or NE–SW compression. Under this regime, the NE faults would act as transfer zones with dominant dextral strike–slip motion and subsidiary normal displacement. This interpretation is in agreement with the work of Mantovani et al. (2002), which demonstrates an E–W compression during the Late Miocene.

3.3. Evidences for meteoric flushing and important fluid/rock interactions

Many geologists have worked on the characterisation of fluid flow, especially in the case of petroleum systems, in order to obtain a precise chronology of the different generations of diagenetic phases as well as to determine the nature/origin of the fluids and water–rock interactions. This characterisation requires an integration of techniques, including: (1) a detailed field survey to establish a primary chronology of the diagenetic features involved. At the same time a thorough field sampling is realised; (2) an accurate petrographical (e.g. classical petrography, cathodoluminescence and fluorescence microscopy, scanning electron microscopy) and geochemical study (e.g. stable isotopes, Sr-isotopes, trace element characterisation by means of electron microprobe analysis) or other techniques (e.g. microthermometry,...) in order to define the different generations of diagenetic phases and to link this to fluid composition and origin. However, often petrographical and geochemical signatures have been reset by later water–rock interactions. Experience learns that, especially in carbonates, addressing the primary nature of the diagenetic products and their related fluids is often very difficult.

In the Ionian Basin, three reservoir analogues located in different thrust units (i.e. Berati, Kurveleshi and Cika units) have been sampled (Fig. 1A) to characterise the fluid flow evolution and the fluid water–rock interactions as well as the main migration pathways for the hydrocarbon fluids during the successive steps of the kinematic evolution of the Albanides FFTB.

In this paper, the case study of the Kelcyra area (i.e. Berati unit) (Vilasi et al., 2006), located in the inner part of the Ionian foothills, is presented as a case study. This case was selected especially since complex water–rock interactions, resulting from the occurrence of salt either as diapirs or along the décollement level, have been determined. A summary of the paragenesis and the characteristics of the main vein fillings (i.e. called cements) are shown on the Fig. 2 and Table 1. Six major stages of fluid cementation have been identified and associated with the FFTB evolution. For each stages, major to trace elements (e.g. Sr, Mg, …) have been determined by the use of Scanning Electron Microscope (SEM), allowing quantitative geochemical analyses of areas as small as 2 μm.

3.3.1. Early meteoric diagenesis

The pre-deformational diagenesis is characterised by the occurrence of a meteoric-derived fluid (Vilasi et al., 2006), which accounted

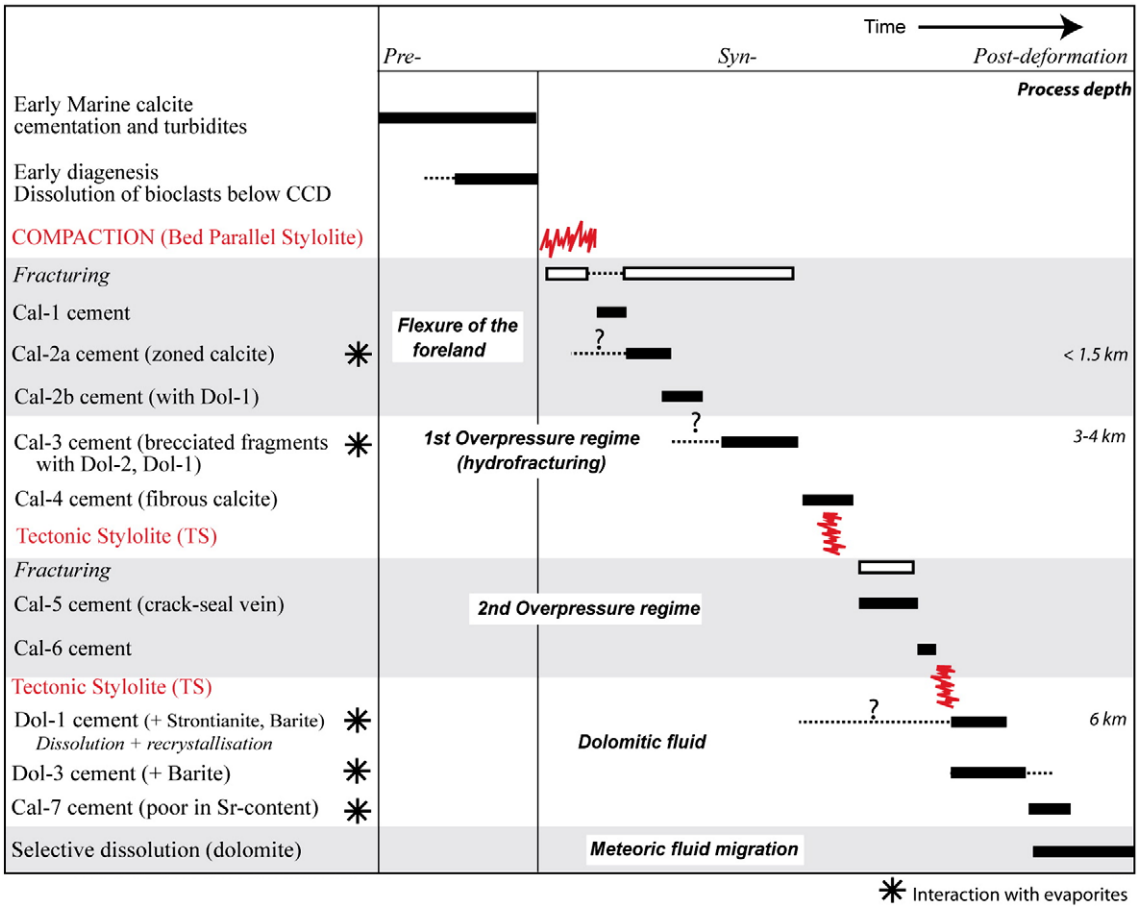

Fig. 2. Paragenesis of Late Paleocene–Eocene deep marine carbonates in Berati unit (Kelcyra area, Albania). The stars in the first column indicate that the cement shows signs of interaction with evaporites.

for the precipitation of Cal-2 cement in N150° oriented fractures (backtilted data) during an extensive phase. The signature of this early fluid has been buffered by a succession of interactions either with rock matrix along its migration pathways or has been affected by interaction with late fluid migration by reopening former veins. Due to this interaction, it is difficult to trace their initial origin and migration pathways, which is essentially based on the presence of some remnants of cements.

Cal-2 calcite cement is characterised by sector-zoned calcite crystals in cathodoluminescence (Fig. 3A and B) and high Sr-content, on average of 3678 ppm. It precipitated during the burial stage from meteoric-derived fluids that is attested by isotopic data. Values are plotting on the meteoric water line (Lohmann, 1988) with rather constant $\delta^{18}O$, varying around −3.2‰ V-PDB and negative $\delta^{13}C$ displaying values from −2 to −6.25‰ V-PDB (Table 1). These results are also consistent with the occurrence of non-metastable one-phase fluid inclusions, which can point to an entrapment below about 40–50 °C (Goldstein, 2001), corresponding to a maximum depth of 1.5 km (cf. geothermal gradients of 21 °C/km). Cal-2 is also characterised by various salinities from 21.9 to 35 wt.% NaCl (Bodnar, 1993), corresponding to T_m (melting temperature) values from −19 to −38 °C.

The precipitation ends with the widespread cementation of calcite, with high Mg-content (values up to 4960 ppm) and slightly lower Sr-content (up to 6960 ppm). This change in the Mg composition points either to an interaction with a later Mg-rich fluid or to a progressive enrichment during its precipitation. At present, the main part of the cement displays intense recrystallisation under CL, where only few remnants of zoned calcite crystals still exist (Fig. 3C). This intense recrystallisation supports the hypothesis of an interaction with a postdating Mg-rich fluid. Moreover a longitudinal dissolution occurs often in the vein, which attests of the migration of a post-Cal-2 corrosive fluid, causing diagenetic alteration, recrystallisation and secondary porosity development. Cal-2 cement contains also many scattered micrometric dolomite crystals (i.e. Dol1), characterised by uniform red-dull luminescence (Fig. 3A and D). These rhombohedric dolomite inclusions precipitated mainly along calcite twins and are usually associated with barite ($BaSO_4$) and acicular strontianite crystals ($SrCO_3$) (Fig. 4D). They have high Sr-content, with an average content of 2963 ppm (Microprobe analyses). The high Sr-content of the dolomite and its association phases, i.e. strontianite and barite, attest of the migration of a fluid that was rich in SO_4^{2-}, Sr^{2+}, Ba^{2+} and Mg^{2+} and not fully undersatured to calcite. It may be explained by an interaction or an expulsion from SO_4^{2-}, Sr^{2+}, Ba^{2+} and Mg^{2+} rich-bearing unit, like evaporites. A second generation of fluid inclusions, located in recrystallised Cal-2, displays T_h (homogenisation temperature) from 95 to 142 °C, which should correspond to the temperature of the fluid responsible to the recrystallisation (Dol1 fluid).

Consequently, two intervals can be proposed in the Ionian Zone, which are the Messinian interval (i.e. in the flysch) and the Triassic unit (along the décollement level or in diapirs). According to the Sr^{87}/Sr^{86}-isotopes, the second hypothesis, explaining an interaction with Triassic evaporites, is retained, since they display similar Sr-isotopic signatures. The geochemical differences in Mg- and Sr- contents in the Cal-2 cement can consequently be explained by fluid–rock interactions between Cal-2 cements and Dol1 phase, resulting in an enrichment in Mg and a depletion in Sr of the Cal-2 cement.

3.3.2. First main compressive stress

Cal-3 (Table 1) precipitates in large N°150 oriented fractures. The calcite cement usually is characterised by the incorporation of

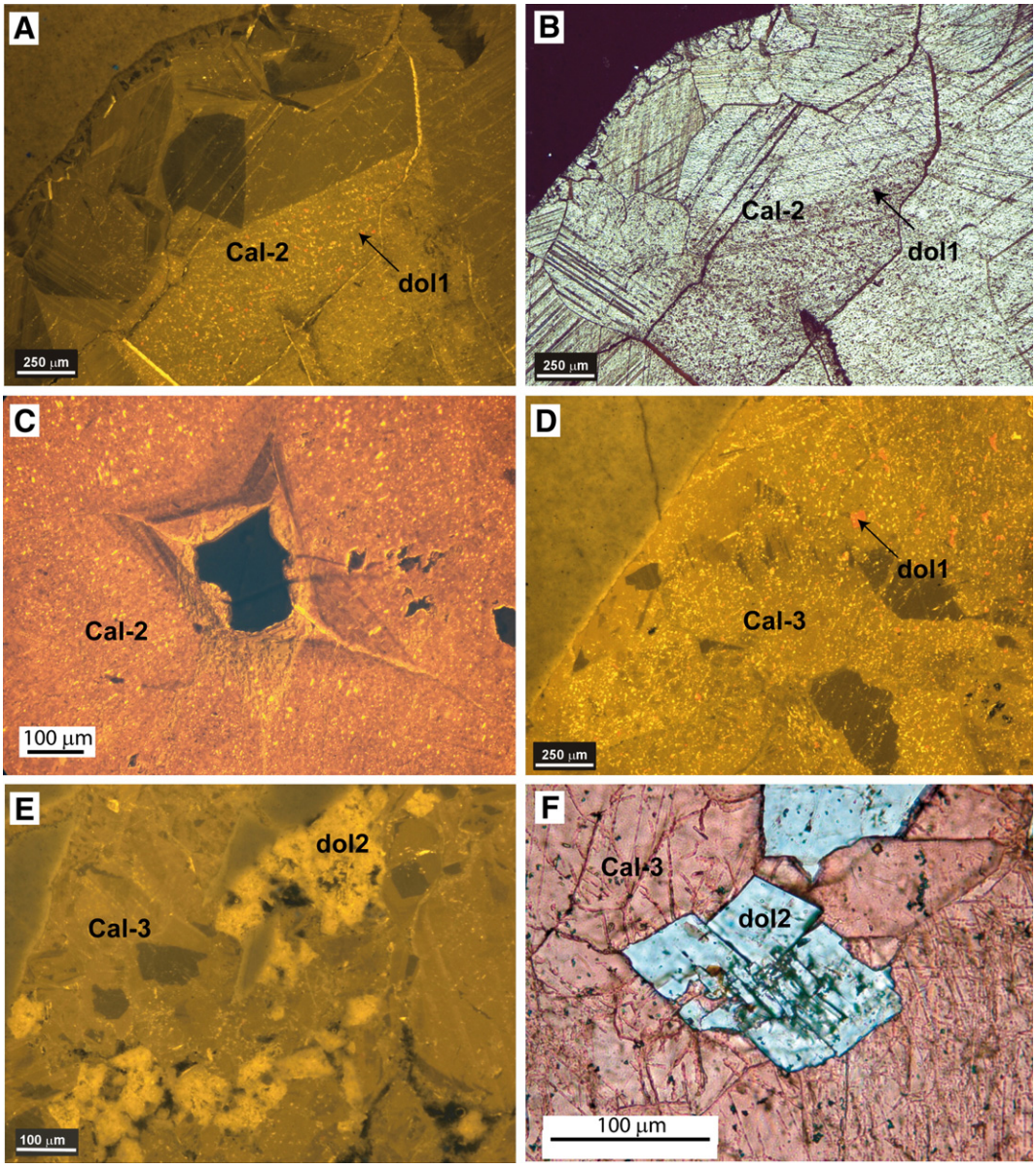

Fig. 3. Thin-section petrography of diagenetic processes: (A) and (B) CL and transmitted light views of Cal-2 vein generation, showing highly twinned calcite crystals and many scattered dolomitic inclusions (red-carmine luminescence, Dol1); (C) CL view of a rest of sector zoned luminescent calcite into the Cal-2 cement; (D) CL view of recrystallised Cal-3 cement, where occurs red-dull luminescent Dol1; (E) CL view of Cal-3 cement, displaying brecciated fragments of partially calcitised dolomites (yellow luminescent, Dol2) in a dull luminescent calcite cement; (F) Transmitted light view of Cal-3 cement, stained in a pink colour (i.e. Alizarin Red-S and potassium ferricyanide) with transported unstained dolomites (Dol2). Note the occurrence of dolomite crystals with altered borders. (For interpretation of the references to colour in this figure legend, the reader is referred to the web version of this article.)

numerous brecciated wall-rock fragments (dolomite Dol-2 crystals; Fig. 3E and F), which are different from the immediate neighbouring vein wall. That suggests that Cal-3 vein formed by hydraulic fracturing during the syn-deformational stage. The brecciated fragments contain transported minerals like phyllosilicates, strontianite, apatite and barite.

Based on fluid inclusion analyses, Cal-3 cement displays an homogenisation temperature T_h varying from 34 to 60 °C and a melting temperature T_m varying between −14 and −32 °C. The latter correspond to salinities from 19 to 30 wt.% NaCl. However, due to the partial recrystallisation of the calcite crystals, the variation in T_h does not allow to determine the original precipitation temperature of the cement. The two end-members of T_h, i.e. 34 an 60 °C, could either be interpreted in terms of different precipitation temperatures or correspond to a partial resetting during the recrystallisation of the calcite (Nielsen et al., 1994). Geochemically, Cal-3 cement has high Sr-content up to 4080 ppm and Mg-content of averagely 2500 ppm. A possible interaction with Triassic evaporite can also be suggested to understand the quantity of Sr and the similarity of their Sr^{87}/Sr^{86} ratio of respectively 0.707777 (Swennen et al., 1999) and 0.707823.

Based on the C- and O- isotope results, the cement displays a $\delta^{13}C$ signature buffered by the host-rock and a $\delta^{18}O$ more depleted, with values ranging from −2.5 to −0.4‰ V-PDB. In vein samples, where brecciated fragments occur, the O-isotopic signature is shifted towards the positive values, between −0.13 and +1.66‰ V-PDB, whereas the $\delta^{13}C$ remains homogeneous.

Based on the C- and O- isotope results, the positive $\delta^{18}O$ signature is of major interest since they attest of a fluid system either influenced by clay diagenesis (Boles and Franks, 1979; Van Geet et al., 2002) or derived from Triassic evaporites during its migration.

As it is the case for Cal-2 cement, Cal-3 cement is also highly recrystallised and characterised by the presence of many scattered

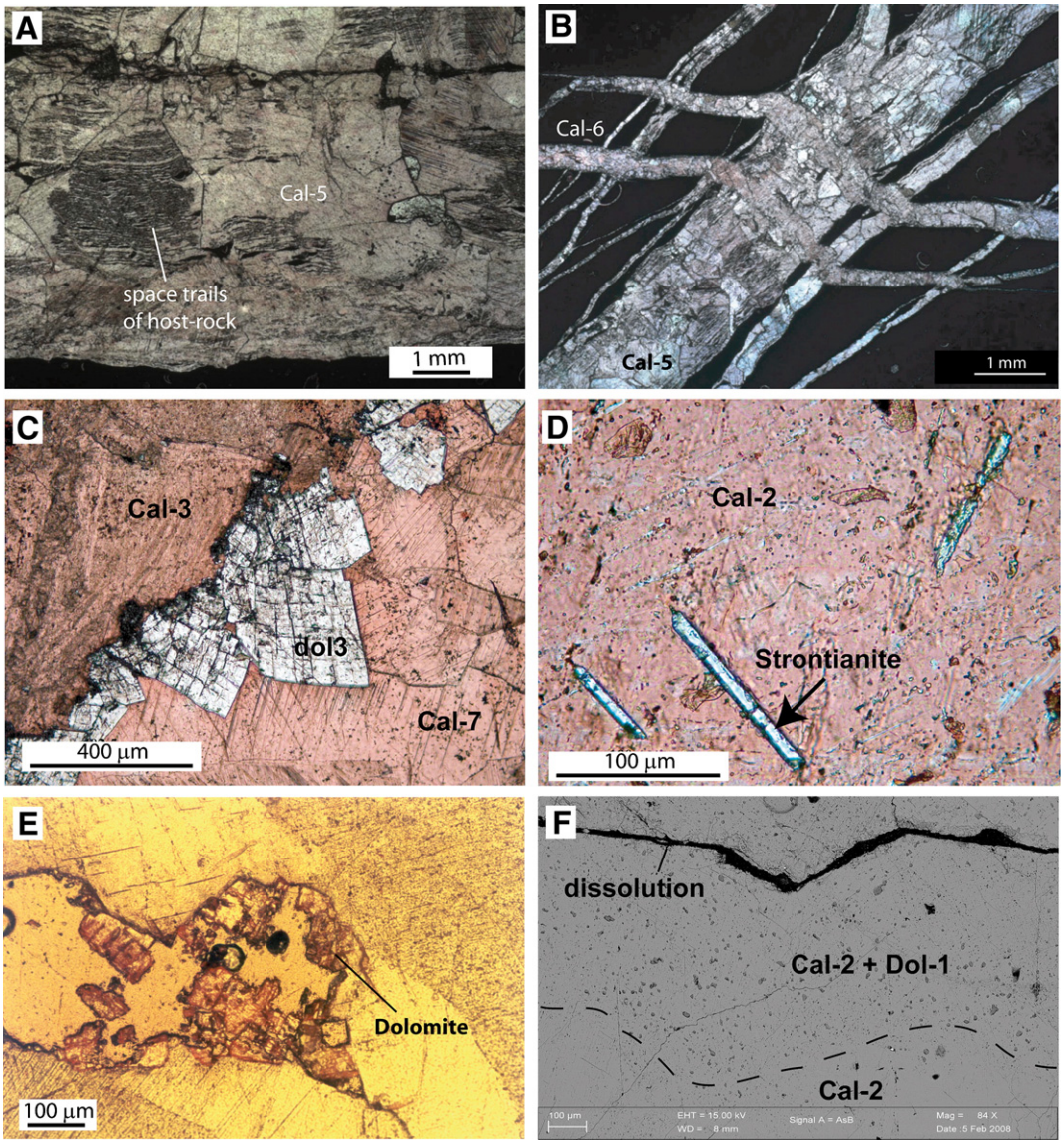

Fig. 4. Thin-section petrography of diagenetic processes: (A) Transmitted light view of the fibrous antitaxial texture of the Cal-5 cement, showing many trails of pieces of wall-rock; (B) Transmitted light view of Cal-5 vein crosscutted by Cal-6 veins; (C) Transmitted light view of Dol-3 cement, which precipitates in re-opened fracture. The unstained dolomite crystals are subhedral. This generation predates Cal-7 cement, which consists of dull sector zoned calcite crystals; (D) Transmitted light view of unstained strontianite crystals occurring in the Cal-2 cement; (E) Selective dissolution of dolomite crystals; (F) Backscattered electron image of Dol1 crystals. It is clear that the dolomite precipitates close to the dissolved area of the Cal-2 vein.

red-dull luminescent dolomite and barite. The latter have the same petrographic and geochemical characteristics than those contained into the Cal-2 cement. They also precipitated close to a central dissolution, developed by post-Cal-3 aggressive fluid migration.

Finally, high salinities and precipitation at low temperature likely under high pressure characterise the Cal-3 cement. During its migration, this fluid has interacted probably with the Triassic dolomite/evaporites, located along the décollement level. This precipitation should have occurred at a depth of 2.5–3 km.

Afterwards, this vein is crosscutted by a corrosive fluid, rich in strontium, barium and sulphate. The latter allows to develop a secondary porosity and a recrystallisation in the hosted cement and precipitate dolomite (Dol-1), barite and strontianite. This latter diagenetic process occurs at minimum 142 °C, which is consistent with a depth of 6 km.

3.3.3. Second compressive stress

The subsequent evolution is defined by a possible second increase of the pressure. Cal-5 cement precipitates after the shear veins (Cal-4; fibrous calcite cement), which developed subsequently to the tectonic stylolites, during the thrust emplacement.

The elongate-blocky calcite crystals of Cal-5 are ferroan, with on average 2193 ppm of Fe, and display a dull luminescence. They have high Sr-content, up to 4870 ppm. Stable isotopes for these veins show negative $\delta^{18}O$ values from −1.48 up to −5.78‰ V-PDB and $\delta^{13}C$ signatures between +1.28 and 1.92‰ V-PDB, that are buffered by the host rock (Table 1). This spread in $\delta^{18}O$ values is interpreted either in terms of precipitation at different elevated temperatures and/or differences in non-equilibrium precipitation temperature between host-rock and fluids or recrystallisation of the cement.

The characteristic features of the Cal-5 cement are the presence of pieces of wall-rock, i.e. inclusion bands, aligned parallel to the vein wall (Fig. 4A and B). These regularly spaced trails are clearly bands of wall-rock detached from the neighboured vein-wall and relates to crack-seal growth (Ramsay, 1980; Cox, 1987; Bons, 2000).

The origin of this fluid cannot yet be determined with the current data. Only few fluid inclusions have been recognised in this cement, most of them being metastable. Cal-5 cement is likely linked with the

generation of overpressures in the front of the tectonic units during the thrust emplacement, which is in agreement with the occurrence of N°150 oriented veins.

Moreover, the timing of this second compressive stress cannot be made more accurate with the available dataset. Consequently, Cal-5 could either originate from the previous recorded overpressure, i.e. Cal-3, or have developed during a second episode of high pressure. Here, the change in the cement composition (Sr and Fe contents) supports the second hypothesis, describing the development of a second compression event.

3.3.4. Transition stage

During the syn-deformational stage, the development of thin fractures is coeval with the migration of marine fluids in the system. Cal-6 vein are cemented by dull luminescent blocky calcites. Here, few amounts of Sr, with on average 255 ppm, and high Mg-content on average of 2425 ppm, compared to the previous vein generations, are determined. Only one isotopic analysis was realised (Table 1), displaying $\delta^{18}O$ and $\delta^{13}C$ values of −2.88‰ V-PDB and +0.82‰ V-PDB respectively. This value is similar to those of the host-rock, which supports a rock buffering system. The origin of this fluid is still unknown, since no stable fluid inclusions were found.

3.3.5. Dolomite phase (Dol-3)

This stage is characterised by the cementation of a subhedral dolomite (i.e. Dol-3, Fig. 4C), defined by slightly curved surfaces. They precipitate in re-opened veins, as encountered in Cal-3 cement. They display double twins and red-dull luminescence. Geochemical analyses reveal that these dolomites have low Sr-content, defined by values below the detection limit. Unfortunately, no fluid inclusions have been encountered in these crystals. However if the recrystallisation of the calcite cement, pointing out in Cal-2 and -3, relates effectively to the migration of the dolomitising fluid, Dol-1, the precipitation temperature of Dol-1 occurred at elevated temperature, about 140 °C.

Only one isotopic analysis was carried out in order to characterise the corresponding fluid. But since the vein is surrounded by other vein generations and is 1.5 mm wide, the sampling is not very phase selective and therefore likely mixed with Cal-7 cement (Fig. 4C). The result of this single measure shows very depleted O-isotope with a value of −7.58‰ V-PDB and a $\delta^{13}C$ signature of 0.26‰ V-PDB. This result can be interpreted as a precipitation at elevated temperature (i.e. deep-sourced fluid origin).

Based on SEM observations, micrometric barite inclusions, with high Sr- and Al-contents, occur scattered in Dol3, pointing probably to the remobilisation of sulphate. This fluid should have highly interacted with or expulsed from an SO_4^{2-}, Ba^{2+} and Mg^{2+}-rich bearing layer, like the Triassic (i.e. along décollement level or in diapirs) or the Messinian evaporites (i.e. in the Peri-Adriatic Depression). Except their distinct content in Sr^{2+}, Dol1 and Dol3 cements display the same petrographic and geochemical characteristics, revealing a likely similar origin. In this way, the initial fluid must have low Sr-content, which is attested by the geochemical analyses performed on Dol-3 cement. Its enrichment, observed in Dol-1, should have occurred by interaction with Sr-rich cements, like Cal-2 or Cal-3, during its migration through the secondary porosity. An overestimation of the Sr-content can also be suggested, since the penetration depth of the microprobe may be higher than the size of the dolomite.

To summarise, a dolomitic fluid, enriched in barium and sulphate, migrated along re-opened veins at elevated temperature and dissolved partially former calcite cements (i.e. Cal-3 and Cal-2 cements). This diagenetic process caused the development of a secondary porosity and induced also a recrystallisation of the former calcite cement. By fluid/cement interaction, the fluid became enriched in Sr (i.e. Dol-1) due to intense interaction with the high Sr-content calcite cement, whereas it precipitated as low Sr-content dolomite (Dol-3) in the fractures. This migration could point to a hydrothermal origin, but additional research is needed to confirm this hypothesis. The second possibility, which can be considered, described the migration of two distinct dolomitising fluids, i.e. Dol-1 and Dol-3, at different moments However, their association with barite and the similar cathodoluminescence signature of the two generations of dolomite support the first hypothesis, describing the migration of a single dolomitising fluid.

3.3.6. Late calcite cement

Cal-7 cement (Fig. 4C) postdates the tectonic stylolites and precipitates in NW–SE and N–S oriented fractures. The cement displays dull sector-zoned luminescence, and is usually associated with brecciated fragments of dolomite (Dol-2 generation). The brecciated fragments are similar to those in Cal-3 cement, but less numerous and smaller in size. In some places, especially along grain boundaries, accumulations of transported fluorite are observed, associated with pyrite and detrital phyllosilicates.

The occurrence of brecciated fragments of dolomite gives a clue for a migration under high pressure regime. The Sr-isotope signature of 0.708039 for Cal-7, which is similar to previous measurements realised on the Triassic evaporites of 0.708010 (Swennen et al., 1999), possibly supports intense interaction with Triassic dolomite interval. However this signature also suggests a Middle Oligocene marine signature, which is characterised by a Sr-isotopic signature varying from 0.707900 to 0.708050 (McArthur and Howarth, 2004).

The positive $\delta^{18}O$ signature of the Cal-7 cement between +0.12 and +1.12‰ V-PDB can also be explained by the intense host-rock buffering with evaporite intervals or by clay diagenesis. Geochemically, Cal-7 cement is as low Sr-, Al-, Si-, and Fe-contents.

This cement can be associated to a fluid, which underwent intense water–rock interaction with evaporites-bearing unit and with Triassic dolomites.

3.3.7. Late dissolution stage

The last stage in the diagenesis is characterised by the development of a possibly subrecent karst system. It caused a selective dissolution of dolomite crystals, as testified by the rhombohedral shape of the moldic secondary porosity (Fig. 4e). Some dolomite crystals however are also replaced by bright yellow luminescent calcite, which points to a dedolomitisation process. This probably occurs at the subsurface, as a telogenetic process, due to the effect of percolation of meteoric water (Chaftez, 1972).

4. The use of calcite twins within veins as paleo-stress and paleo-burial indicators

4.1. Aim and method

This part of the study aims at placing constraints on the tectonic framework of paleofluid flows in the vein systems observed in the folds of the southern Outer Albanides. No detailed microtectonic analysis had been made previously to constrain the timing of fracture development in the foreland and to accurately characterise the related paleostress orientations and regimes, in relation with the regional tectonic evolution. The ultimate purpose was therefore to bridge the gap between geochemical analyses at the local scale and regional-scale tectonic history, through the analysis of mechanical twins within the calcite cements filling the veins. Combining this approach with the study of microstructures observed in the field and at the scale of the samples allowed to establish a chronology between vein formation/cement crystallisation (and hence the timing of fluid flows within these veins) and development of the frontal folds.

Calcite twin analyses have been widely used to constrain both the structural and kinematic evolution of fold–thrust belts, e.g., Sevier and Appalachian forelands: Craddock and Van Der Pluijm, 1999; Northern Pyrenean foreland: Rocher et al., 2000; Southern Pyrenean foreland:

Holl and Anastasio, 1995; Gonzales-Casado and Garcia-Cuevas, 1999; Subalpine chain: Ferrill and Groshong, 1993; Taiwan: Lacombe et al., 1993; Rocher et al., 1996; Hung and Kuo, 1999; Hudson valley fold–thrust belt: Harris and Van der Pluijm, 1998; Zagros: Lacombe et al., 2007. These studies have led to regionally significant reconstructions of tectonic stress and strain patterns, and, in few cases, to the quantification of differential stresses associated with folding and thrusting.

Twinning in calcite occurs at low temperature and requires a low critical Resolved Shear Stress (RSS) of 10 +/−4 MPa that depends on grain size (e.g., Rowe and Rutter, 1990; Lacombe and Laurent, 1996) and internal twinning strain (e.g., Turner et al., 1954; Laurent et al., 2000). Calcite twinning is not sensitive to either strain rate or confining pressure, and therefore fulfils most of the requirements for paleopiezometry.

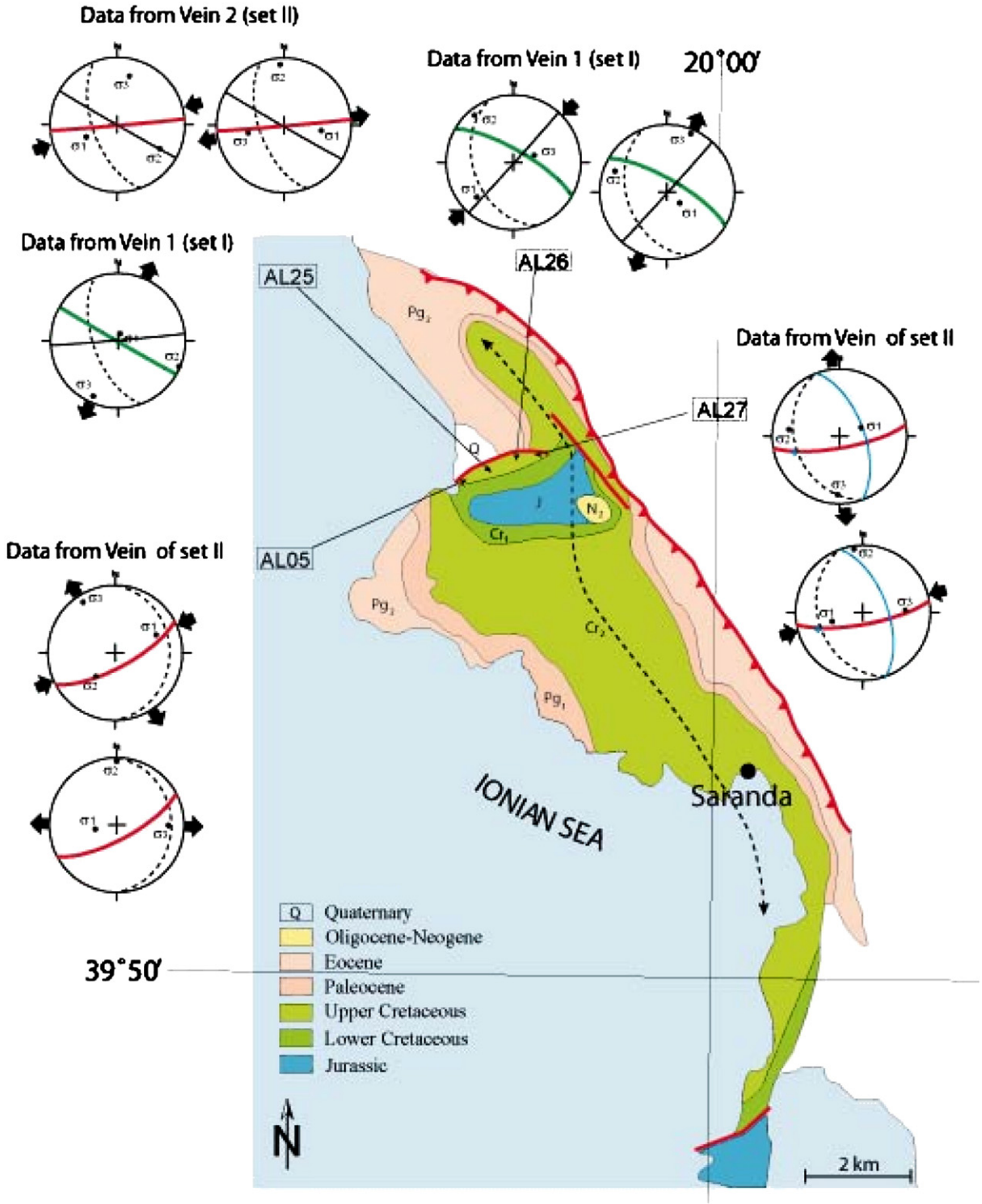

Fig. 5. Detailed map of Saranda anticline with reported paleostress orientations determined from calcite twin analysis. Stereodiagrams: Schmidt lower hemisphere, equal area projection. Bedding as dashed line; in each diagram, the vein in colour (green, set I; red: set II) is the vein from which the stress tensor has been determined. (For interpretation of the references to colour in this figure legend, the reader is referred to the web version of this article.)

Calcite twin data being basically strain data, Groshong's (1972) strain gauge technique is commonly used to produce a strain ellipsoid, while differential stresses are given by the Jamison and Spang (1976) technique. In this paper, we used the Etchecopar method of inverting calcite twin data (Etchecopar, 1984; see details in Lacombe, 2001) that computes simultaneously stress orientations and differential stress values and is, therefore, the only technique to date that unambiguously relates differential stress magnitudes to a given stress orientation and stress regime. This method applies to small twinning strain that can be approximated by coaxial conditions. Therefore, orientation of twinning strain can be correlated with paleostress orientation (Burkhard, 1993).

The inversion process takes into account both twinned and untwinned planes, the latter being those of the potential e-twin planes which never experienced a RSS of sufficient magnitude to cause twinning. The inverse problem consists of finding the stress tensor that best fits the distribution of twinned and untwinned planes. The orientations of the 3 principal stresses σ1, σ2, and σ3 are calculated, together with the Φ ratio [$\Phi = (\sigma 2 - \sigma 3)/(\sigma 1 - \sigma 3)$] and the peak differential stresses (σ1–σ3) sustained by rocks. If more than ~30% twinned planes in a sample are not explained by a unique stress tensor, the inversion process is repeated with the uncorrelated twinned planes and the whole set of untwinned planes. Where polyphase deformation has occurred, this process provides an efficient way of separating superimposed twinning events (e.g., Lacombe et al., 1990).

4.2. Sampling and measurements

As mentioned earlier (Section 3.2.2), two main vein systems have been identified in the Saranda and Kremenara anticlines (Fig. 1A). The first set (I) is oriented N140° ($^{+}/-20$), and likely predated folding. This set developed during burial, possibly in response to high fluid pressure (Section 3.2.2). The second set (II) is oriented N60° ($^{+}/-20$) and is likely a vein system formed in response to the regional compressional stress responsible for folding. In both folds, pervasive pressure solution is evidenced by widespread stylolitisation.

Oriented samples were collected from homogeneous, poorly deformed, marine limestone of late Cretaceous age, cut by the above-mentioned vein systems. The fine-grained facies of these limestones did not enable us to carry out analysis of calcite twins within the rock matrix, so only four samples from the western flank of the Saranda anticline (AL05, AL25, AL26 & AL27; Fig. 5) were available for calcite twin analysis. An additional sample from the Kremenara anticline has been studied in order to allow comparison with results from Saranda. Thin twins are dominant in the samples, indicating that calcite deformed below 200 °C (Burkhard, 1993; Ferrill et al., 2004) (Fig. 6). Twinning strain never exceeds 3–4%.

Sampling in fold limbs allowed to constrain the chronology of twinning relative to folding. For example, one might expect that if a twin set formed during Layer-Parallel Shortening (LPS) and was subsequently tilted with the strata during folding, then one axis of the stress tensor should be perpendicular to bedding with the other two lying within the bedding plane. In contrast, late/post folding twin sets should yield two horizontal stress axes and one vertical one, within a range of 10° uncertainty. Examination of abutting/cross-cutting relationships between veins and bedding-parallel/tectonic stylolites, together with collection of twin data in crosscutting set I and set II veins, also helped to constrain the chronology of twinning events.

4.3. Results: paleostress orientations and regimes and relation to vein development and regional fold–thrust belt evolution

Despite the low number of samples available for this study, calcite twin analysis consistently revealed the main states of stress in both Saranda and Kremenara anticlines. The first stress regime corresponds to a N70° compression and a sub-perpendicular extension. The different tensors related to this stress regime are linked by stress

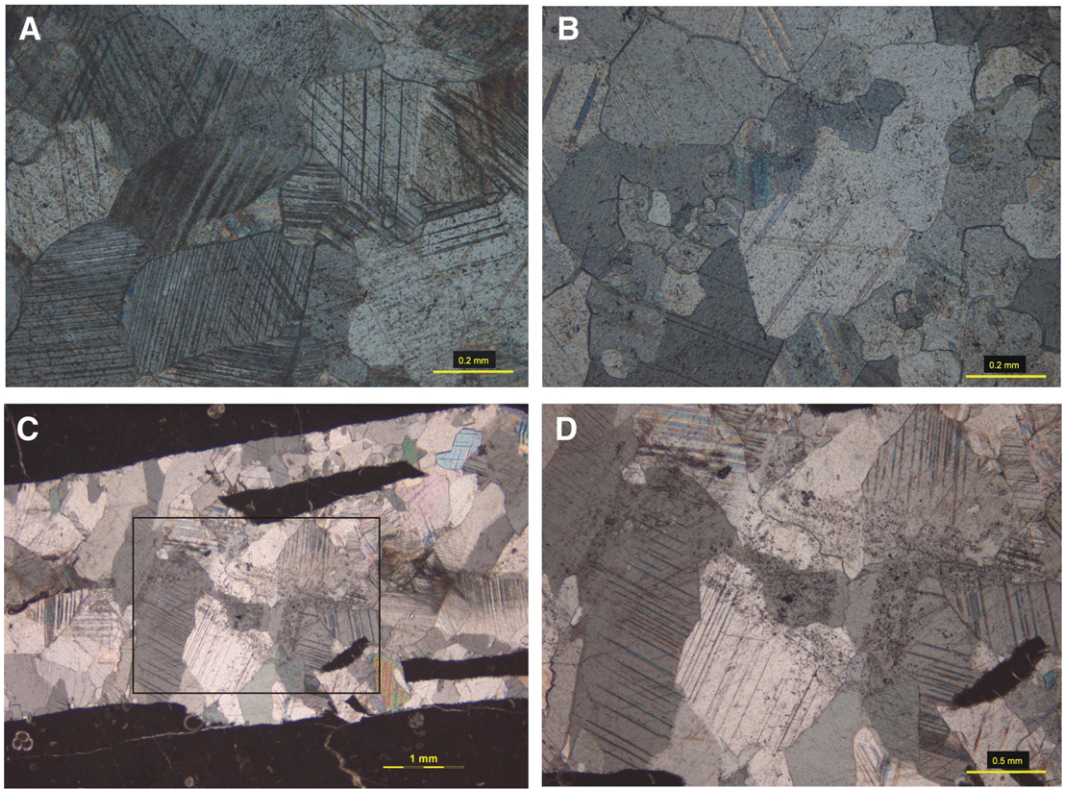

Fig. 6. Examples of twinned calcite crystals in veins from the Saranda anticline. A: AL25 sample, high twin density; B: Al27 sample, low twin density. C, D: DR10 sample. Note that twinning occurred in the thin twin regime in all samples, suggesting low strain recorded at low (<200 °C) temperature (Burkhard, 1993; Ferrill et al., 2004).

permutations: after backtilting, σ1 is either horizontal, with σ2 or σ3 trending N160°, or vertical and associated with a N160° trending σ3 (Fig. 5). This stress regime accounts well for the formation of set II veins and associated tectonic stylolites. The attitude of the computed stress axes with respect to bedding reveals that twinning recorded LPS in the samples from Saranda and late stage fold tightening in the sample from Kremenara; the N70° compression, that lies at high angle to fold axes, therefore likely prevailed during the entire folding history.

The second stress regime corresponds to a pre-folding nearly E–W extension, perpendicular to the local N–S trend of the Saranda anticline (Fig. 5); it likely reflects outer-rim extension during fold development. The third stress regime also prevailed before folding; it corresponds to a N30°-directed extension, which is likely responsible for the opening of the early set I veins in response to the flexure of the foreland in front of the advancing thrust sheets, contemporary with burial and possibly under high fluid pressures.

4.4. Results: from differential stress values to paleoburial

Lacombe (2007) has shown that paleo-differential stress against depth suggests a trend of increasing differential stresses with depth, supporting that stress in the upper crust is mostly at frictional equilibrium, in agreement with contemporary stress measurements (Townend and Zoback, 2000). For given stress and pore pressure regimes, and knowing the differential stress values from calcite twin analysis, one can make use of this relationship to estimate the paleodepth of deformation. Fig. 7 reports the curves of differential stress values as a function of depth in a crust in frictional equilibrium, for strike–slip (SS) and reverse faulting (*C*) stress regimes, values of λ [$\lambda = P_f/\rho gz$, where P_f is the pore fluid pressure, ρ the density of the overlying rocks, g the acceleration of gravity and z the depth] of 0.38 (hydrostatic) and 0 (dry) and for values of the friction coefficient μ of 0.6 and 0.9.

We focused on stress tensors related to the regional compression that has been recorded either at the very early stage (LPS) or at the very late stage of folding (fold-tightening). Extensional stress tensors were not considered. Reporting the differential stress values corresponding to reverse, strike–slip or mixed reverse/strike–slip (i.e., with low Φ ratio) stress regimes related to the N70° regional compression on the above-mentioned curves yields the probable range of depths at which Cretaceous limestones recorded twinning strain. In Saranda, the depth range of the investigated samples just before the onset of folding (i.e., at the maximum burial) was about 1.5–5.5 km, around a mean value of 4 ± 1 km that represents the most likely burial depth of these limestones.

These preliminary paleodepth estimates, although scattered and possibly overestimated (see discussion in Lacombe, 2007), are consistent to a first-order with other independent paleoburial indicators. Although the thicknesses of sedimentary formations in the Ionian zone are poorly constrained, at least 2000–2500 m of Paleogene (including the Oligocene flysch) can be considered above the Cretaceous limestones (e.g. Collaku et al., 1990). Muska (2002) estimated from Genex-1D modelling a thickness of eroded rock of nearly 1600 m above Eocene formations. In addition, taking into account a thermal gradient of about 16–20°/km (e.g., Roure et al., 2004), and paleotemperatures between 40 and 60° derived from microthermometry of paleofluids, the possible depth range is about 2–4 km, consistent with our estimates from calcite twins. Additional constraints are provided by the maturity rank of the organic matter in the Mesozoic series sampled in surface outcrops of the Ionian Basin and Kruja Zone: Ro values for Toarcian samples were found lower than 0.55 and, therefore, the rocks are immature (Roure et al., 1995); Ro values lie between 0.7 and 0.9 for the late Triassic. Taking into account the low geothermal gradient, these Mesozoic limestones were

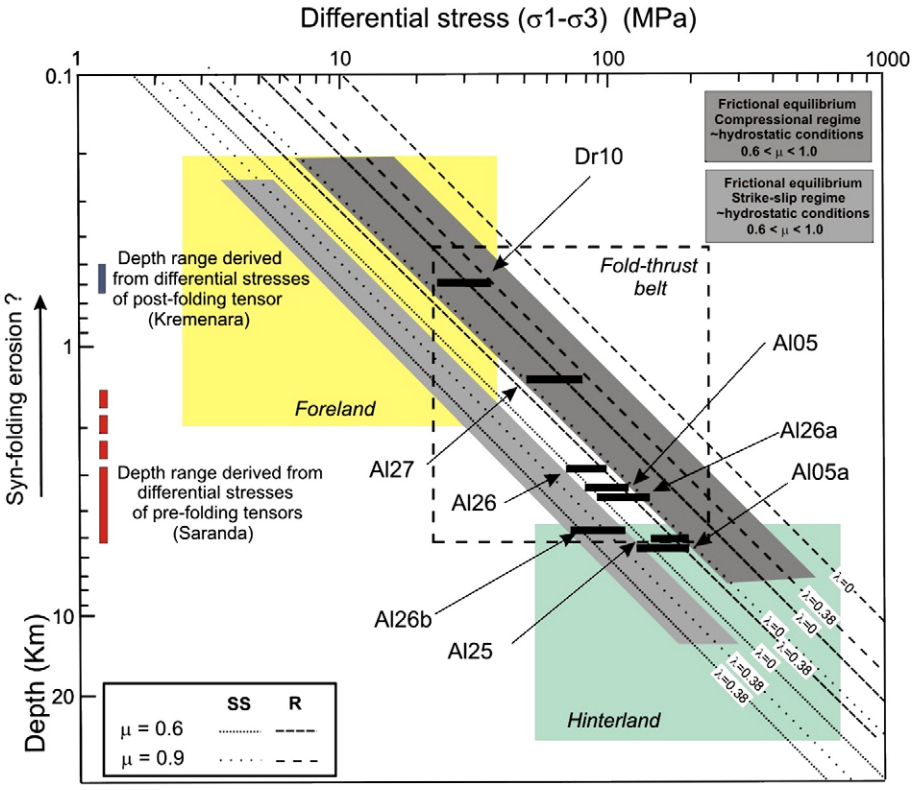

Fig. 7. Differential stress values determined from calcite twins reported on stress/depth curves built for a crust at frictional stress equilibrium (Lacombe, 2007), and derived paleoburial values for pre-and post folding stress tensors. Labels a and b refer to stress estimates obtained from subsets of twin data of homogeneous grain sizes, while others were obtained from the whole data set in each sample.

probably never buried to depths greater than 4 km, in agreement with our estimates.

In the Kremenara anticline, the post-folding differential stress values correspond to a depth of 0.5–0.6 km. Assuming that the maximum burial was nearly the same than in Saranda, this may indicate an erosion of ~3 km at the crest of the anticline during folding. Note, however, that these two tectonic units (i.e. Cika belt and Kurveleshi belt) have different evolutions and are therefore not directly comparable, so further studies should confirm these conclusions.

5. Coupled 2d-stratigraphic, kinematic, thermal and fluid flow modelling

Before performing a coupled thermal and fluid flow modelling, a good knowledge of the basin scale structural geometry and history is needed. This begins by the construction of regional structural balanced cross-sections with lithological attributes, representative of the present-day deformation state of the studied area. In this study, the present-day cross-section was built using geological maps, well data (ages, lithologies and seismic velocities from well logs and cuttings) and depth-converted interpreted seismic data. In the Albanides, the seismic data provide also a strong control on the architecture of pre-, syn- and post-kinematic strata and their space-time relationships with faults and folds. These observations permit to sequentially retrodeformed the present-day cross-section and reconstruct intermediate deformation states.

5.1. Coupled Thrustpack–Dionisos forward kinematic and stratigraphic modelling (Input templates for Ceres)

The 2D kinematic evolution of the Albanian studied section was modelled with the Thrustpack software that uses an algorithm based on the kink-band method for fold-bend fold of Suppe (1983). The Thrustpack simulations consist of performing a series of forward time steps to reproduce successive deformations (faulting, folding and flexure) on the basis of the geological restored cross-sections (Sassi et al., 2007; Sassi and Rudkiewicz, 1999). In this software, the observed geometry of the syntectonic deposits and of the fault paths into them is drawn at each stage before to apply the tectonic offsets. Former strata located above erosional unconformities are then erased before initiating the next kinematic stage. Finally, the software calculates the compaction in the section between two deformation steps, depending on the lithologies given by the user for each new sedimentary layer. A reasonably good fit to the observed section geometry can be obtained in this way, in spite of the restrictions imposed by the fold-bend fold model. There is however no real constraint on the topographic profiles reproduced into the Thrustpack modelling, except those approximated from the geological profile and the distribution of sand/shales.

The 2D stratigraphic evolution of the Albanian studied sections was also modelled with the Dionisos software. The Dionisos software is a multi-lithological dynamic-slope forward computer model that uses deterministic physical laws to simulate the transport of sediments in 3D (Granjeon and Joseph, 1999). In the Dionisos simulations, the interactions between three main processes (accommodation, sediment supply and sediment transport) are numerically solved at each time step. The changes of accommodation are linked to the basin deformation, induced by tectonic movements and sediment loading, the sea level variations and the sediment compaction. The supply of sediments can be an inflow coming from the erosion of adjacent source areas (i.e. clastic sediments), or an in-situ production controlled by ecological rules and physical parameters such as water depth and wave energy (carbonates). The transport of sediments is simulated using two sets of water-driven diffusive equations, in order to reproduce the interaction between the long-term fluvial and gravity transport, and the shorter-term transport induced by catastrophic floods, slope failures and turbiditic flows. The numerical quantification of the interactions between accommodation, sediment supply and sediment transport leads to a 4D (x, y, z and t) model that represents the evolution of the stratigraphy and the topography of the studied area trough time.

As many other stratigraphic computer model, Dionisos was first developed to simulate the vertical tectonic movements that are a component of the accommodation space. Although it can now reproduce some horizontal displacements such as listric normal growth faults, it is not yet able to reproduce such tangential offsets repeating layers as thrusting. This is why a newly developed coupling between the Thrustpack and the Dionisos softwares was tested in this Albanian study.

The coupled kinematic and stratigraphic modelling consists in an exchange of data between the two softwares, each one supplying the other one with complementary information (Albouy et al., 2003a,b) (Fig. 8). At the end of each kinematic stage, Thrustpack thus exports towards Dionisos the initial topography and lithologies of the model surface, as well as its vertical displacement vectors corresponding to the underlying thrusting, folding and flexural deformation. On the basis of these inputs, Dionisos incrementally performs a simulation of the accommodation changes, the sediment supply and the sediment transport on the duration of the same kinematic stage. Dionisos then sends back to Thrustpack a template for the final topographic profile of the stage, which in that case takes into account the physics of the erosional and depositional processes. Incremental Thrustpack kinematic stages can finally be performed again using the new information on the topography and if needed, on the lithologies also calculated by Dionisos for the syn-tectonic deposits between the wells data. At the end of this computation, the structural, stratigraphic and topographic knowledge of the area is considerably improved and the final geometric results of the Thrustpack modelling can be ultimately used as intermediate boundary conditions/templates for a regional 2D coupled thermal and fluid flow modelling using the Ceres software as described below.

5.2. Fluid flow modelling

Basin-scale modelling techniques are required to understand the velocity and trends of fluid migrations, pore fluid pressures, temperature evolution of the basin and the hydrodynamic behaviour of faults. The Ceres software is a 2D-basin modelling that allows to model sedimentary basins and understand the petroleum systems in complex structural environments, such as salt-driven tectonic areas, diapirism and foreland-fold-and-thrust-belts, where blocks are displaced along faults (Schneider, 2003; Schneider et al., 2002).

In addition to the simulation of overpressures, Ceres software is able to model the formation and evolution of the petroleum system by reconstructing the hydrocarbon generation and migrations but also to trace the changes in the water flow through time. In this way, a link between the thermal evolution, the fluid pathways, the diagenetic processes and the deformation history is required to replace the fluid migrations within the kinematic evolution.

5.2.1. Work flow

To carry out such study, the work flow operates with three main steps (Schneider et al., 2002), which are the edition of the initial section, the restoration of the section and finally the forward simulations:

(i) The initial section can be edited on the screen or using a template geometry imported directly from another study or other softwares such as Thrustpack (i.e. the final section that is equivalent to Present Day geometry). At this stage, it is recommended to use a structural software that is able to balance the section, such as Locace, 2D Move, Restore or 2D-

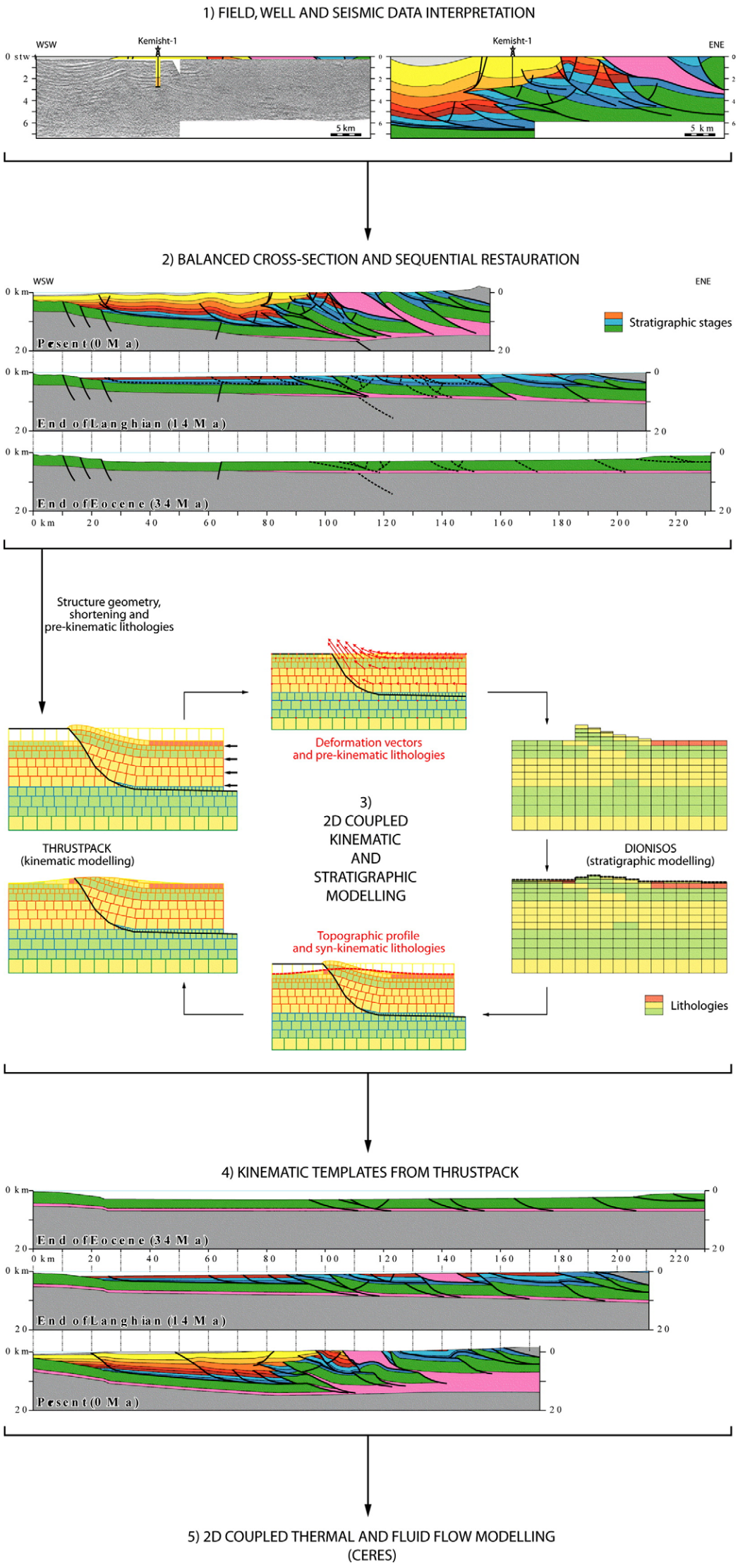

Fig. 8. Workflow of the coupled structural/stratigraphic forward modelling. For explanation see text.

GeoSec softwares (Gibbs, 1983; Moretti et al., 1988; Moretti and Larrère, 1989; Tozer et al., 2006). The geological attributes are then assigned, including the horizons, faults, décollement levels, section boundaries, the age of the horizons and finally the lithologies, which may evolve spatially but not in time. The sub-domains are subsequently defined as small independent kinematical units or blocks. The meshing, which is specific for each block, is built with no constraint coming from the other blocks. Geometrically, the initial section holds the Brittle Upper Crust as well as the Ductile Lower Crust and the Moho (Fig. 9).

(ii) The section is then restored with a backward process, where the intermediate geometries built with Thrustpack are directly used as templates in Ceres to rebuild the eroded parts and to perform the displacements along faults. Once the erosion and the sedimentation are accounted for, the resulting section is uncompacted using porosity-depth relationships. At this stage, the displacement along individual faults is applied using translations and vertical shear (version 4.0). As for the edition of the eroded parts, this operation may be facilitated by the use of templates as it was the case for the present study.
Once the thickness is restored, the last step of the backward simulation requires the correction of local inconsistencies in the computed thicknesses that result from the use of the vertical shear mode of deformation. The correction of the eroded part may be also done at this stage. However, this step allows mainly to account for salt or mud tectonics and diapirism as well as thickness modifications. These steps were done for each layer of the initial section at present day. The final scenario of the restoration was then validated using input data derived from former kinematic studies.

(iii) The last step is a forward modelling coupling the fluid flow simulations, the heat transfer, the hydrocarbon formation, the compaction and pore space evolution, the building up of overpressure, etc. To solve the problems of permeability and pore saturation in complex tectonic setting, Ceres defines several sub-domains, the boundaries of which being mainly defined by faults and model boundaries. The principal equations are mass conservation of solid and fluids (cg. 3 phases: water, oil, gas), coupled with Darcy's law and compaction law (Schneider et al., 2002).

Three options have been implemented to handle the permeability and long term behaviour of the faults. Faults can either be assumed as pervious (i.e. first option) or impervious (i.e. second option), being then considered as a flow barrier. Alternatively their permeability can also evolve through times according to the neighbouring lithologies (i.e. third option). Permeability can also change with the strain rate. Whichever option is chosen, the faults are considered as inactive when their velocities are lower than the defined speed limit of 50 m/Ma.

In the framework of this study, the three options have been modelled but only the second option, where the permeability is dependant to the lithologies on both sides, is illustrated in detail. A quick comparison with the two other options, considering the faults as either impervious or pervious, will be carried out.

5.2.2. Kinematic scenario

The kinematic evolution of the Albanides is strongly influenced by the occurrence of the Triassic evaporites, deposited during the rifting stage. The east-trending studied transect cross the Albanides from the Peri-Adriatic Depression in the west to the Kruja Platform in the east. This section crosses also the Vlora-Elbasan transfer zone, where all the major Albanian oil fields occur (Fig. 1A).

This fluid flow modelling was used to study essentially the impact of the faults on the fluid migration, to determine whether they acted as fluid barriers or drains, to quantify the fluid flow, and to reconstruct the pore fluid pressure history of the subthrust reservoirs. The resulting scenario, modelled with Ceres, is illustrated in the Fig. 10 and demonstrates successive major kinematic episodes, based on the work previously done by Barrier et al., 2003, 2005:

- end of the passive margin during the Oligocene (−23.7 Ma), with active folding in the internal Albanides and flexuring of the foreland basin which was subsequently filled by the Oligocene flysch.
- thrust emplacement of the Kruja belt, resulting in the flexuring and turbiditic sedimentation in the Ionian Basin during the Aquitanian (−20.52 Ma).
- onset of the thrusting in the Ionian zone during the Langhian (−13.7 Ma).
- out of sequence thrusting, accounting for the development of an intermediate tectonic unit in the Ionian Basin (i.e. Berati belt) during the Serravalian (−11.6 Ma).
- maximum shortening of the Ionian zone during the Tortonian (−7.5 Ma), causing an important flexural subsidence in the foreland. At the same time, the eastern most thrust units were already uplifted and eroded.
- burial increases related to thrusting and coeval synorogenic sedimentation in the foreland increased the flexural subsidence. The compressive front was still active and many compressive structures were growing in the foreland during the Messinian (−5.3 Ma).
- the present day profile shows partial erosion of the Oligocene seals located at the top of the tectonic units that allows the unroofing and emersion of the main reservoir interval in the Kruja and Berati belts.

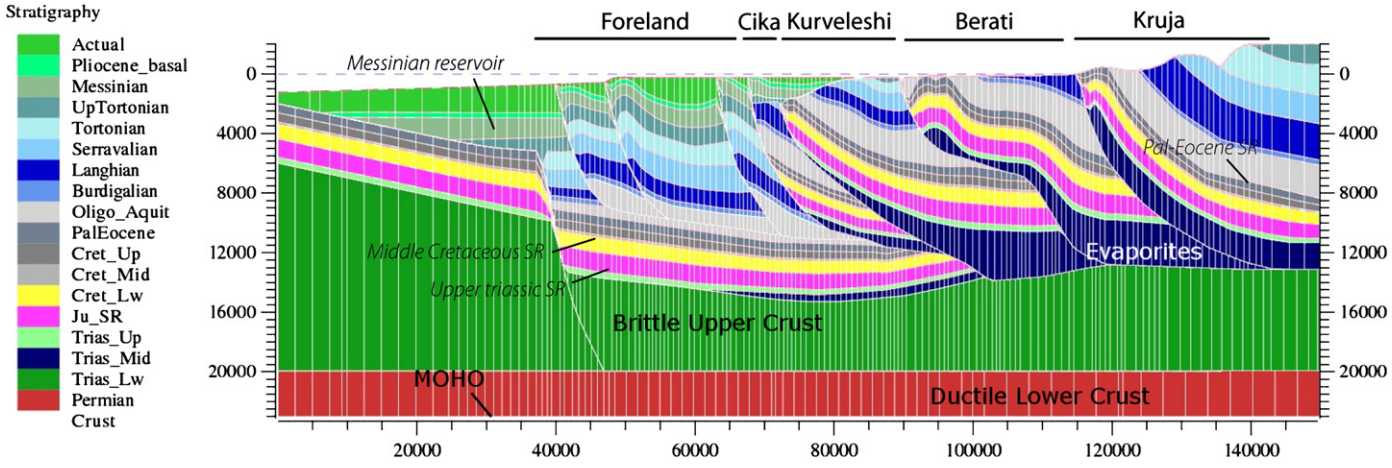

Fig. 9. Geometry and lithology distribution of the section at present day. The three main source rocks (SR) are located in the section.

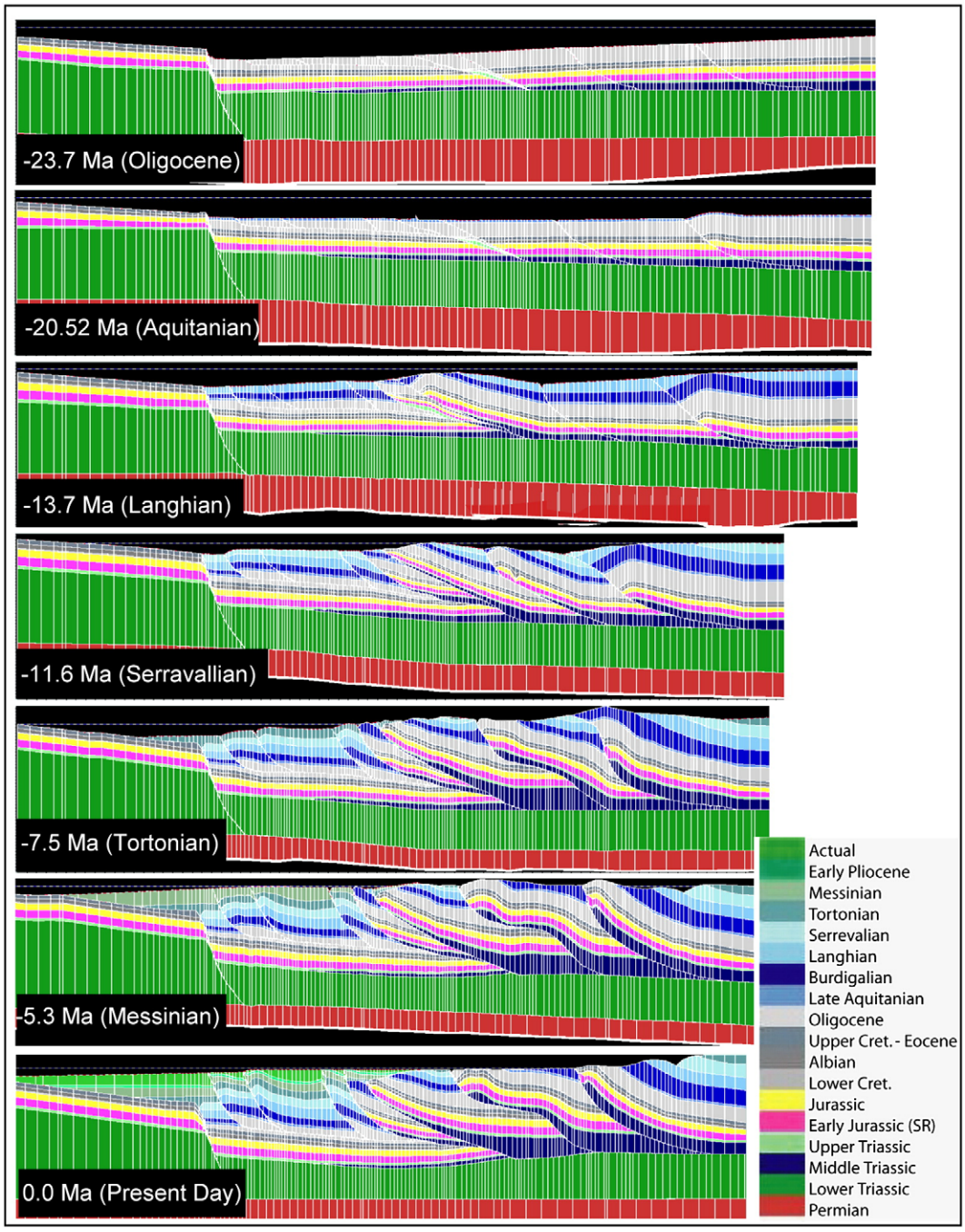

Fig. 10. Kinematic evolution of the Ceres model along the studied CR 13 section (Fig. 1) from the Late Oligocene (−23.7 Ma) to present day.

For this modelling, three organic-rich source rock formations have been considered (Mattavelli et al., 1991; Curi, 1993; Speranza et al., 1995; Rigakis and Karakitsios, 1998): a) the Upper Triassic–Lower Jurassic blackshales, which are the main effective source rock, with TOC values up to 5,5%; b) the Middle Cretaceous bituminous shale and limestones with 2,5% of TOC; and c) the Paleocene–Eocene shaly limestone in the Kruja belt, where the TOC reached 4,5%. Their organic matter is types I to II marine origin.

As previously described, carbonate reservoirs range in age from Upper Cretaceous to Eocene and essentially consist of pelagic facies of the Ionian Zone, characterised by a dual fracture–matrix porosity. Their reservoir characteristics are largely enhanced by the presence of numerous open fractures. Other reservoir intervals, located in the Peri-Adriatic Depression, such as the Pliocene and Messinian sandstones, are also oil-bearing.

The trapping mechanisms have a dominant stratigraphic control that must account for the seal capacity of the Oligocene flysch and the Messinian evaporites. However, in places where the Oligocene flysch has been tectonically removed, the Triassic evaporites along the decollement level also constitute a composite stratigraphic and structural seal, i.e. in the Delvina oil field.

5.2.3. Thermal calibration

Accurate forward structural modelling allows a direct control on the burial history of source rocks in foreland fold–thrust belt systems. However, one of the most important steps in the fluid flow modelling is the thermal calibration of the section, in order to predict a realistic evolution of the source rocks, the timing of hydrocarbon generation and expulsion and the possible way of hydrocarbon migration between the sources to the traps. Many paleothermometers can be

used along the profile, such as Bottom Hole Temperature (BHT), present-day heat flow, geothermal gradients, as well as petrophysical and laboratory data such as Vitrinite reflectance, Apatite Fission Tracks, microthermometry and Rock-Eval analyses. Even if the present temperature of buried reservoirs can be easily calibrated since this parameter is not too sensitive to its fluctuation through time, the difficult step remains to determine the best evolution of the heat flow in order to obtain an accurate present day maturity repartition.

In the case of foreland-fold–thrust belts, the evolution of the heat flow, which occurs during the sedimentary filling of the flexured basin, is very difficult to determine, since folding and thrusting stages are often associated with important sedimentation rates (i.e. flysch deposition). The intense flexuring may imply a blanketing effect for the thermal evolution due to slow sediment compaction. It is usually followed by an important subsidence (i.e. the filling of the accommodation space) during the maximum shortening (Barrier et al., 2003, 2005). For this study, different hypotheses on the heat flow variation have been tested, especially to determine the importance of the blanketing effect and to constrain better the model.

In the Albanides, low geothermal gradients exist at Present, ranging from 16 to 20 °C km^{-1} (Cermak et al., 1996; Frashëri, 2005) with generally an increase towards the east. These values are associated with anomalous heat flow values as low as 30 to 40 mK m^{-2}, with unclear distribution. In some places, strong variations of the temperature gradient are also observed mostly due to the complex tectonic structures in the vicinity of salt diapirs (high conductivities), transfer zones (i.e. Vlora Elbasan lineament) and local reversal in temperature gradient due to meteoric circulation and karsts. For this study, the heat flow variation used to model the fluid flow, corresponding to the best fit with the actual data, is described on the Fig. 11.

5.3. Fluid flow

Source rock maturity is estimated either by the vitrinite reflectance values (Easy Ro; Ardic, 1998), or through the transformation ratio (TR) that represents the advancement of the transformation of kerogen into hydrocarbon. This has been computed for the three source rocks previously described.

5.3.1. Maturation vs. kinematic evolution

According to fluid flow modelling, sedimentary burial was already sufficient during the Late Oligocene to already mature the Triassic source rocks in the still subsiding Ionian basin (Fig. 12A). Alternatively, shallower source rocks, i.e. the Toarcian and the Middle Cretaceous blackshales, remained largely immature in the Ionian Basin and the Paleocene–Eocene shaly limestones of the Kruja platform until the Tortonian episodes of the deformation (Fig. 12B), when tectonic burial ultimately forced them to enter the oil window.

At the present-day (Fig. 12C), the Upper Triassic–Jurassic source rocks are overmature in the foreland, whereas in the thrust units they are still mature or in the condensate-gas window. Only the top of the Kurveleshi belt is still immature, since this unit uplifted at the onset of thrusting and consequently always remained at lower temperature.

The Middle Cretaceous source rock is principally mature to immature in the Ionian tectonic units from the base to the top of the tectonic units respectively, whereas the maturity of the Paleocene–Eocene shaly limestone of the Kruja unit is higher and has reached the gas-condensate window.

Finally, the model shows two main steps of maturation: the first one during the sedimentary burial, which allows the Triassic source rock to enter the oil window as early as the Oligocene and to increase the maturity of the shallower source rocks. Afterwards, during the syn-deformational stage, thrusting will help to keep the source rocks of allochthonous Ionian units in the oil window and to progress slowly towards the condensate-wet gas window, whereas source rocks are overmature in the foreland since the Late Tortonian.

The variation in maturity between the Berati–Kruja belts and the Kurveleshi–Cika belts can be explained by the development of out-of-sequence thrusting during the Albanides evolution, allowing an increase of the source rock maturity for the tectonic units that have been uplifted later.

5.3.2. Water saturation

The water saturation has been modelled since it is complementary to the oil saturation. The Fig. 13 shows the oil accumulation in present day, in the case of light oil migration (oil density of 33° API). The known oil-bearing reservoirs are accounted for by the model, but other untested reservoirs, such as the Triassic dolomites, sealed by the Triassic source rock according to the model results, could also account for interesting accumulations with oil saturation higher than 45%.

A more realistic fluid flow modelling would require the input of the true oil density. Unfortunately, different types of oil, in terms of density, have been recovered in Albania, whose degrees API fluctuates

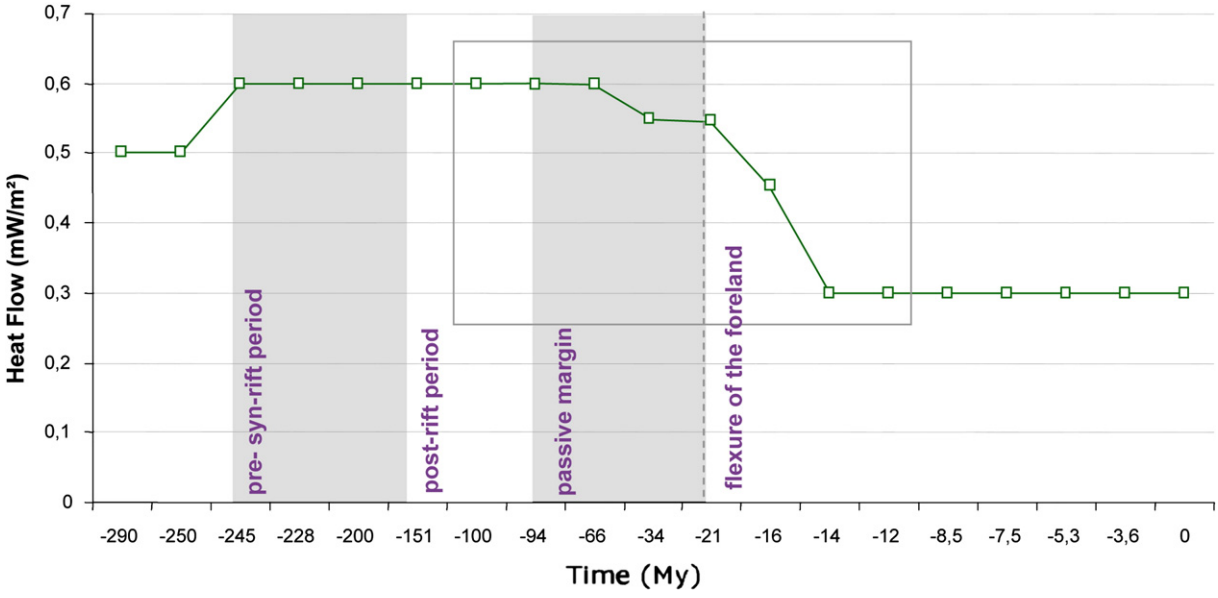

Fig. 11. Determined heat flow variation through time for the studied E–W transect.

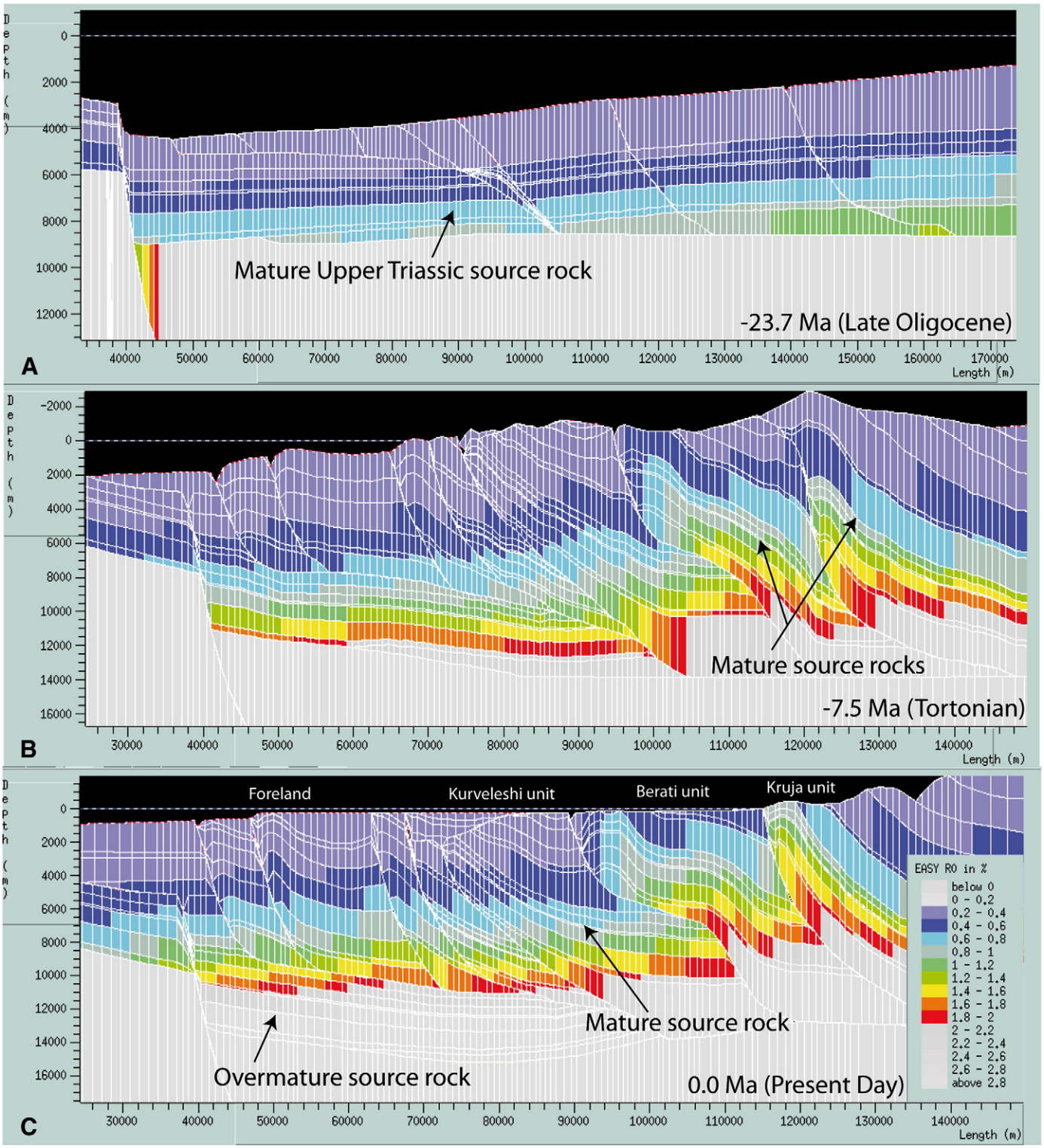

Fig. 12. Repartition of the maturity (Vitrinite reflectance in %) along the CR 13 profile at (A) the Late Oligocene, (B) Tortonian and (C) present day.

in a range between 9 to 37 °API corresponding to densities from 840 to 1000 kg.m-3.

Hence, the migration has been simulated for the two main oil densities (i.e. 33 and 16° API) to clarify whether these two types of oil have been expulsed from the different source rock, or if this density variation relates to late diagenetic processes such as biodegradation or secondary cracking of the hydrocarbon. Several parameters and model results point towards the biodegradation of the hydrocarbon in a post-deformational stage, since the migration of heavy oil would not be able to reach the known reservoir intervals and because the amount of free hydrocarbons in the samples remains too high (i.e. Rock-Eval pyrolysis) to have been subjected to a secondary cracking. This is in agreement with the single burial stage observed in the Ionian Zone.

5.3.3. Migration pathways as a function of the fault behaviour

The pre-deformational stage is characterised by early generated hydrocarbons, which migrated vertically up- and down dip as early as the Oligocene until the Burdigalian. During this early migration stage,

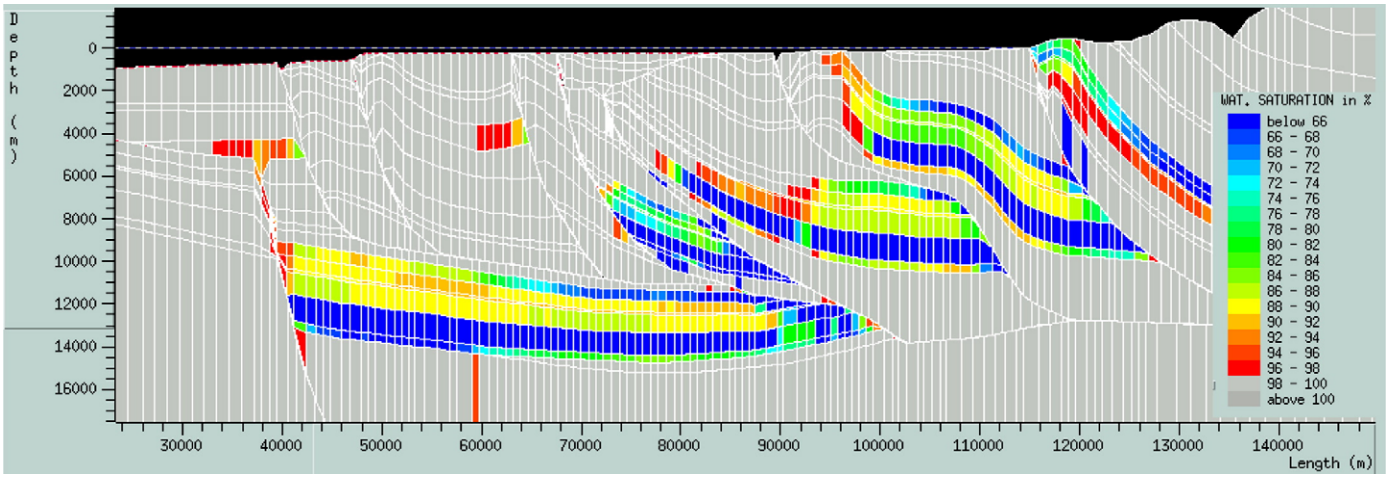

Fig. 13. Water saturation at the present day. Note that the decrease in water saturation is complementary to the oil saturation.

developing during the foreland flexuring, the main faults acted as fluid conduits allowing the oil of the Triassic source rock to be trapped in the reservoirs of the Kruja unit.

The syn-deformational stage is still characterised by up- and down dip vertical migrations but accounts also for east- and westward migrations in the foreland, particularly towards the Italian offshore. This is attested by direct oil-source rock correlations in the Aquila field, which relates to a distal Triassic source (Albpetrol, 1995). The specificity of the period is a change in the fault behaviour. The presence of evaporites along the décollement level enables to block the oil migration through the faults, even if FFTB evolution and the strain rate would rather predict that they should be pervious during such period. Alternatively, hydrocarbon migration is required along faults in the Cika unit for reaching the sandstone intervals of the foreland and the Italian offshore, where no evaporites exist.

From the Tortonian onward, the hydrocarbons were trapped in the Upper Cretaceous–Eocene fractured carbonate reservoirs. This period is characterised by the major expulsion and migration of hydrocarbon in connection with the maximum shortening and thermal burial.

Since the Messinian (Fig. 14), the migrations are relatively short and partly up- and down dip vertical but other important pathways are east and downward (i.e. reflux). This period is characterised by a shift of the hydraulic head from the thrust belt toward the foreland, where many compressive structures are formed. The later allows a change in the faults behaviour, from fluid conduits in the foreland to fluid barriers in the thrust belt. The evolution of the compressive stress enables to develop oil reservoirs in the foreland, i.e. in the Messinian oil-bearing sandstones. Finally, the sealed faults have completely compartmentalised the fluids within the thrust belt, isolating independent volumes of rocks since the onset of the orogeny.

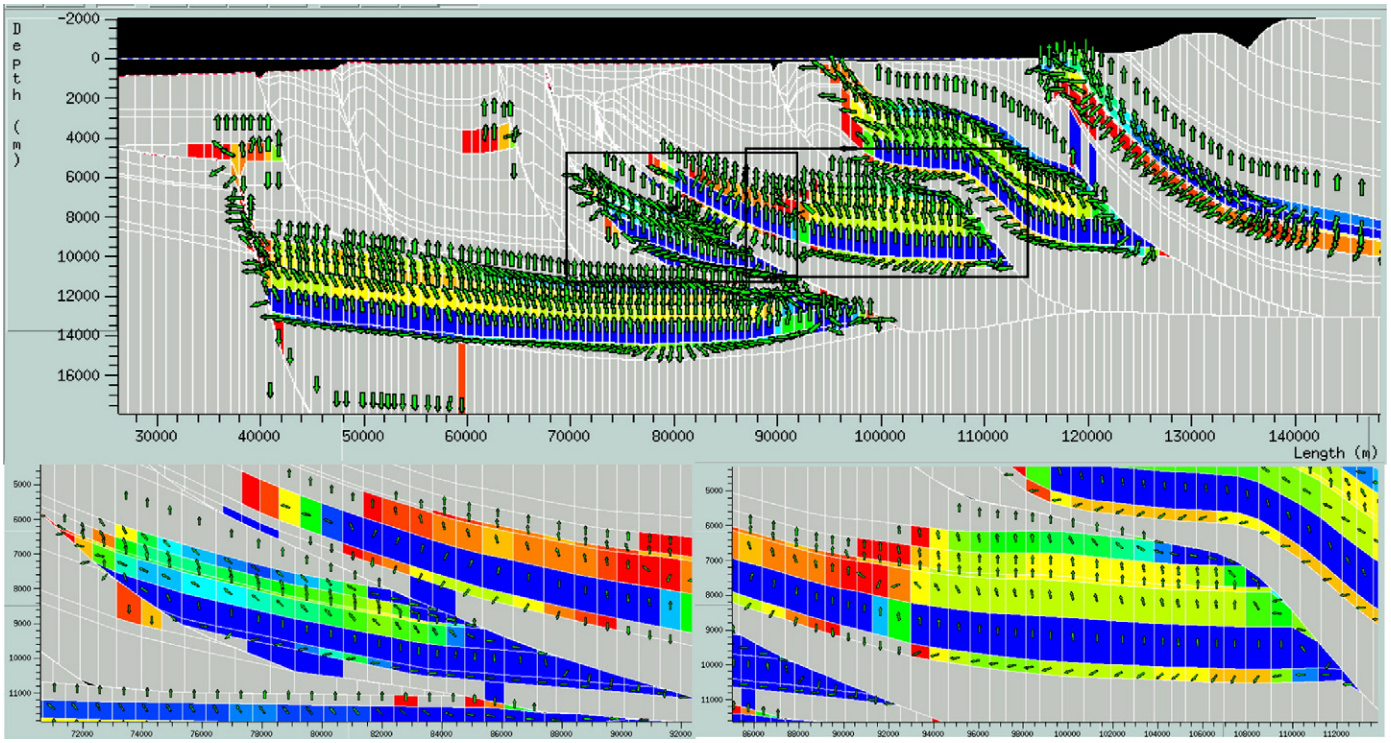

Fig. 14. Water saturation and hydrocarbon migration at the present day with two detailed zones: the Cika unit on the left and the Kurveleshi unit on the right inside. Note the accumulations of hydrocarbon in the Upper Cretaceous to Eocene carbonates located beneath the thrusts, sealed by Triassic evaporite and Oligocene flysch.

These results of fluid flow modelling account for the hypothesis of fault permeability being dependant from the neighboured lithologies (i.e. third option). When considering that the faults are pervious (i.e. first option) all along the FFTB evolution, the fluid migration remains unchanged. In fact, the occurrence of evaporites along the décollement level stops the migration pathways of fluids along the faults. However, when considering the second option, i.e. the hypothesis with impervious faults, results are quite different especially in the foreland, where reservoirs can no longer be charged by hydrocarbons, as they become isolated from the kitchen areas.

6. Conclusions and perspectives

The present paper illustrates an integrated workflow for carbonate reservoir characterisation, coupling kinematic, fluid characterisation and thermal evolution of a fold-and-thrust belt system and associated foreland basin, which has been developed to improve our knowledge of the petroleum system and predict the exploration risks in complex tectonic systems (overpressures, evaporitic diapirs, important erosions …). Such multi-scale study, from outcrop and petrography to basin-scale fluid modelling, could be performed in Albania, which constitutes a unique natural laboratory for the study of active processes in an emerged tectonic wedge. This regional integrated petrographic and basin modelling approaches could precise the timing of deformation and erosion, of the cementation and dissolution episodes, the velocity of the fluids and their evolving chemistry during migration, giving evidence of important water–rock interactions.

The main diagenetic processes are dependent on the fracture characteristics (orientations…) and the fluid flow, e.g. fracture opening, fluid velocity, vicinity to main faults, allowing either large influx of exotic water or instead precluding rock interactions,... Once the different diagenetic episodes of a specific reservoir have been identified, basin modelling can help to validate possible scenarios, based on thermal evolution and faults behaviour, evolving through time, and to replace the characterised fluids (i.e. oil and water) into the kinematic evolution of the FFTB.

In the Albanides, the fracturing of the reservoir intervals has a pre-folding origin (Fig. 15A), whereas the first recorded cement infill has a meteoric origin, implying downward pathways of meteoric water from surface to the Eocene deep marine limestones at the onset of forebulge development. During its migration, this fluid interacts highly with Triassic evaporites, allowing its enrichments in strontium. Regarding the low temperature of precipitation, reaching only 40–50 °C, this meteoric fluid must have reacted with evaporitic diapirs at the surface or sub-surface to finally precipitate at a maximum depth of 1.5 km.

From this stage onward (Fig. 15B), the maximum principal stress becomes horizontal due to tectonic compression. The majority of the fluid generated in the Ionian Zone migrated under high pressure regime, accounting for the occurrence of brecciated fragment with Triassic dolomite, crack-seal veins (Fig. 15C) and attesting also for intense fluid–rock interactions with the Triassic rocks (i.e. near diapirs or along the basal décollement level).

This period is also characterised by two stages of tectonic stylolites development that must be linked to the main thrusting episodes, i.e. the thrust emplacement of the Kurveleshi belt and the out-of-sequence development of the Berati unit. The fluids, which migrated with brecciated fragments during an overpressured regime, precipitated at low temperature, at a depth of 3 km. Afterwards the tectonic burial increased due to overthrusting of the Berati unit by the overlying Kruja unit, the temperature of precipitation becoming higher. This stage is characterised by the development of hydrofracturing and is likely coeval with maximum burial of the Berati belt.

The following stage corresponds to upward migration of sulphate-enriched fluids (Fig. 15D), derived again from Triassic evaporites–dolomites, along the décollement level, which acted as a conduit for deep sourced fluid or the Late Messinian interval. The velocity of this saline fluid flow along the décollement level should be higher than through the fractures, allowing a precipitation in thermal disequilibrium. This period accounts for the onset of the thrusting in the Ionian Zone, and consequently for its associated uplift.

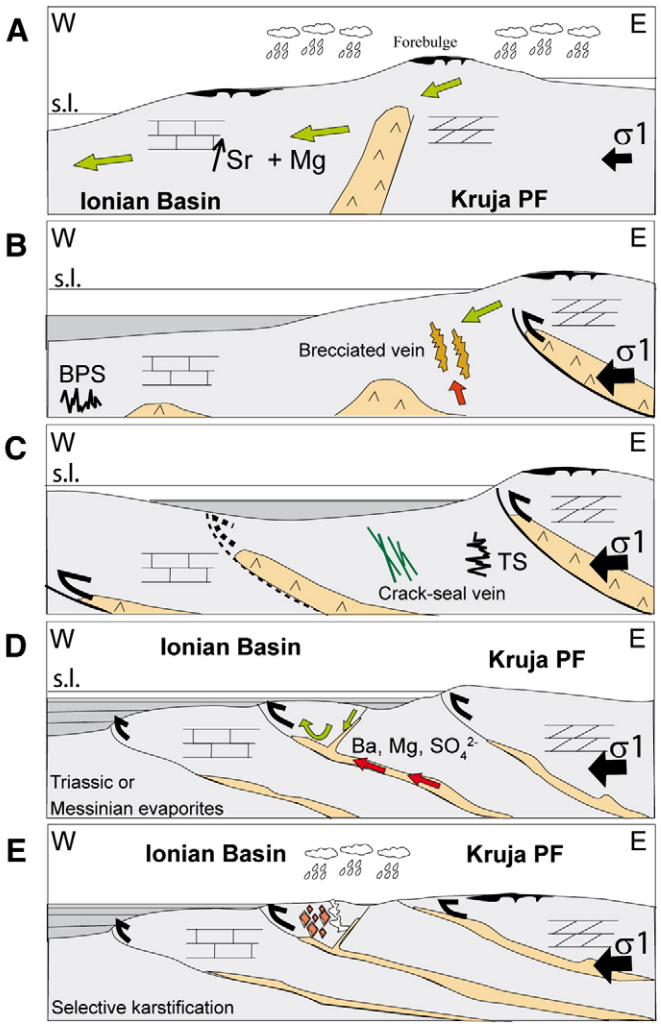

Fig. 15. Conceptual model for the diagenetic study (s.l. = sea level; BPS = Bedding Parallel Stylolites; TS = Tectonic Stylolites). The green arrows show the downward migrations, whereas the red arrows illustrate the upward migrations. (For interpretation of the references to colour in this figure legend, the reader is referred to the web version of this article.)

The last stage is characterised by the migration of meteoric fluids along fractures during emersion, which results in the formation of a selective dissolution of a part of the euhedral dolomites and a partial dedolomitisation of the others (Fig. 15E).

Concerning the petroleum system, we have demonstrated that only light oil (33°API) from Mesozoic source rocks (Toarcian source) migrated since the Langhian onward, ultimately reaching the Upper Cretaceous–Eocene reservoir interval in Tortonian times (i.e. maximum shortening). At Present, the hydrocarbons in place are highly biodegraded, certainly due to important meteoric fluid migrations during post-folding stage, which is in agreement with the chemistry of cemented fractures.

An important result of the Ceres modelling, however, relates to the fault permeabilities. In fact, the main generations of fluids, which were petrographically and geochemically characterised during this study, account for intense fluid–rock interaction with the Triassic evaporites, located either in diapirs (during the pre-deformational stage) or along the décollement level. According to the fluid flow modelling, the faults act principally as flow barriers during the FFTB development due to

the occurrence of evaporites (non-permeable), except in the foreland, where there is no evaporite. Ultimately, some contradictions still exist between observations and modelling results, which point towards the current limitations of the software, as local fractures and successive changes in their porosity–permeability properties related to diagenetic processes, which are not taken into account.

Such coupling of the paleofluids characterisation with the water flow modelling would be required in any other FFTB to document properly the fluid flow history and to get a better prediction of their fluid–rock interactions and overall reservoir characteristics.

Acknowledgements

We would like to acknowledge our colleagues from Albpetrol and the former Oil and Gas Institute in Fieri, especially MM. Ajet Mezini, and Ilia Fili, who provided a constant support for the field studies. We thank also Herman Nijs for preparing the thin sections, Michael Joachimsky for the stable isotopic analyses, Jacques Wautier for the microprobe analyses, Hervé Devoitine, Catherine Marquer and Isabelle Faille for their constant and essential computing support with Ceres modelling.

References

Albpetrol, 1993. Petroleum exploration opportunities in Albania: 1st onshore licensing round in Albania. Publicity brochure, Western Geophysical, London, vol. 12.

Albpetrol, 1995. Recent developments in exploration and oil production and the future in the free market economy. 1965–1995, 30 years Oil and Gas Institute, pp. 23–26.

Albouy, E., Barrier, L., Bonjakes, S., Eschard, R., Guri, S., Muska, K., Rudkiewicz, J.L., 2003a. Tectonique et sédimentation des Albanides centrales. IFP-QKSHH-Albanian Petroleum Institute report. 57657, 55 pp.

Albouy, E., Casero, P., Eschard, R., Barrier, B., Rudkiewicz, J.L., 2003b. Coupled structural/stratigraphic forward modeling in the Central Apennines. AAPG Annual Convention, May 11–14, 2003, Salt Lake City, Utah.

Ardic, C., 1998. Quantitative basin modeling, hydrocarbon generation and migration history of the Moose Mountain Area, Rocky Mountain Foothills, Alberta. PhD Thesis, Univ. Calgary.

Bakiaj, H., Bega, Z., 1992. Lushnje-Elbasan transversal fault as an important feature of the external Albanides—an interpretation. 4th EAPG Conf. and Tech. Exhibition, Paris.

Barrier, L., Albouy, E., Guri, S., Rudkiewicz, J.L., Bonjakes, S., Muska, K., Eschard, R., 2005. Coupled structural and sedimentary mass balances in the Central Albanides. Soc. Géol. de France, Soc. Geol. España, ILP Conference, Thrustbelts and foreland basins, Paris, December 2005, Abs., pp. 47–49.

Barrier, L., Guri, S., Albouy, E., Bonjakes, S., Rudkiewicz, J.L., Muska, K., Eschard, R., 2003. Tectonique et sedimentation dans les Albanides centrales. Intern IFP report, IFP-RB30, QKSHH, 55p.

Benchilla, L., Guilhaumou, N., Mougin, P., Jaswal, T., Roure, F., 2003. Reconstruction of paleoburial history and pore fluid pressure in Foothills Areas: a sensitivity test in the Hammam Zriba (Tunisia) and Koh-I-Maran (Pakistan) ore deposits. Geofluid 3, 103–123.

Bodnar, R.J., 1993. Revised equation and table for determining the freezing-point depression of H_2O–NaCl solutions. Geochimica and Cosmochimica Acta 57 (3), 683-384.

Boles, J.R., Franks, S.G., 1979. Clay diagenesis in Wilcox sandstones of Southwest Texas; implications of smectite diagenesis on sandstone cementation. Journal of Sedimentary Research 49 (1), 55–70.

Bons, P.D., 2000. The formation of veins and their microstructures. In: Jessell, M.W., Urai, J.L. (Eds.), Stress, Strain and Structure: A Volume in Honour of W.D. Means Journal of the Virtual Explorer, vol. 2. 2000.

Bouma, A.H., 1962. Sedimentology of some Flysch Deposits: A Graphic Approach to Facies Interpretation. Elsevier. 168 pp.

Breesch, L., Swennen, R., Vincent, B., 2006. Dolomite formation in breccias at the Musandam Platform border, Northern Oman Mountains, United Arab Emirates. Journal of Geochemical Exploration 89 (1–3), 19–22.

Breesch, L., Swennen, R., Dewever, B., Mezini, A., 2007. Deposition and diagenesis of carbonate conglomerates in the Kremenara anticline, Albania: a paragenetic time marker in the Albanian foreland fold-and-thrust belt. Sedimentology 54, 483–496.

Burkhard, M., 1993. Calcite twins, their geometry, appearance and significance as stress–strain markers and indicators of tectonic regime: a review. Journal of Structural Geology 15 (3–5), 351–368.

Cazzola, C., Soudet, H.J., 1993. Facies and reservoir characterization of Cretaceous–Eocene turbidites in the Northern Adriatic. In: Spenser, A.M. (Ed.), Generation, Accumulation and Production of Europe's Hydrocarbon III: Eur. Assoc. Petrol., Geosciences, pp. 191–207.

Cermak, V., Krest, M., Kucerova, L., Safanda, J., Frasheri, A., Kapedani, N., Lico, R., Cano, D., 1996. Heat flow in Albania. Geothermics, 25 1, 91–102.

Chaftez, H.S., 1972. Surface diagenesis of limestone. Journal of Sedimentary Petrology 42, 325–329.

Cloetingh, S., Topo-Europe team, 2005. Topo-Europe-4D topography evolution in Europe: uplift, subsidence and sea level rise. Geophysical Research Abstracts 7 EGU-05-A-08529.

Collaku, A., Cadet, J.P., Melo, V., Bonneau, M., 1990. Sur l'allochtonie des zones internes albanaises: mise en évidence de fenêtres à l'arrière de la nappe ophiolitique de la Mirdita (Albanie). Comptes Rendus de l'Académie des sciences, Paris, 2 311, 1251–1258.

Cox, S.F., 1987. Antitaxial crack-seal microstructures and their relationship to displacement paths. Journal of Structural Geology 97, 779–787.

Craddock, J.P., Van Der Pluijm, B., 1999. Sevier–Laramide deformation of the continental interior from calcite twinning analysis, west-central North America. Tectonophysics 305, 275–286.

Curi, F., 1993. Oil generation and accumulation in the Albanian Ionian basin. In: Spencer, A.M. (Ed.), Generation, Accumulation and Production of Europe's Hydrocarbons. European Assoc. Petrol. Geosc., Spec. Publ., vol. 3. Springer, Oxford, pp. 281–285.

De Paola, N., Collettini, C., Trippetta, F., Barchi, M.R., Minelli, G., 2007. A mechanical model for complex fault patterns induced by evaporite dehydration and cyclic changes in fluid pressure. Journal of Structural Geology 29, 1573–1584.

Dewever, B., Breesch, L., Mezini, A., Swennen, R., 2007. Sedimentological and marine eogenetic control on porosity distribution in Upper Cretaceous carbonate turbidites (central Albania). Sedimentology, 54 2, 243–264.

Etchecopar, A., 1984. Étude des états de contraintes en tectonique cassante et simulation de déformations plastiques (approche mathématique). Unpublished thèse de Doctorat-ès-Sciences, Univ. Sciences et Techniques du Languedoc, Montpellier, 270 pp.

Ferket, H., Roure, F., Swennen, R., Ortuno, S., 2000. Fluid migration placed into the deformation history of fold-and-thrust belts: an example from the Veracruz basin (Mexico). Journal of Geochemical Exploration 69–70, 275–279.

Ferket, H., Swennen, R., Ortuno, S., Roure, F., 2003. Reconstruction of the fluid flow history during Laramide foreland fold and thrust belt development in eastern Mexico: cathodoluminescence and $\delta^{18}O$–$\delta^{13}C$ isotope trends of calcite-cemented fractures. Journal of Geochemical Exploration 78–79, 163–167.

Ferket, H., Swennen, R., Ortuño Arzate, S., Roure, F., 2006. Fluid flow evolution in petroleum reservoirs with a complex diagenetic history: an example from Veracruz, Mexico. Journal of Geochemical Exploration 89 (1–3), 108–111.

Ferrill, D.A., Groshong, R.H., 1993. Kinematic model for the curvature of the northern Subalpine Chain, France. Journal of Structural Geology 15, 523–541.

Ferrill, D.A., Morris, P., Evans, M.A., Burkhard, M., Groshong, R.H., Onasch, C.M., 2004. Calcite twin morphology: a low-temperature deformation geothermometer. Journal of Structural Geology 26 (8), 1521–1529.

Frashëri, A., 2005. Geothermal regime and hydrocarbon generation in the Albanides. Petroleum geoscience 11, 347–352.

Frasheri, A., Nishani, P., Bushati, S., Hyseni, A., 1996. Relationship between tectonic zone of the Albanides, based on results of geophysical studies. In: Ziegler, P.A., Horwath, F. (Eds.), Peri-Tethys Memoir 2: Structure and Prospects of Alpine Basins and Forelands. Mem. Musee Hist. Nat. Paris, vol. 170, pp. 485–511.

Gibbs, A., 1983. Balanced cross-section construction from seismic sections in the areas of extensional tectonics. Journal of Structural Geology 5, 153–160.

Goldstein, R.H., 2001. Fluid inclusions in sedimentary and diagenetic systems. Lithos 55, 159–193.

Gonzales-Casado, J.M., Garcia-Cuevas, C., 1999. Calcite twins from microveins as indicators of deformation history. Journal of Structural Geology 21, 875–889.

Graham-Wall, B.R., Girbaces, R., Mesonjesi, A., Aydin, A., 2006. Evolution of fracture and fault-controlled fluid pathways in carbonates of the Albanides fold–thrust belt. AAPG Bulletin 90, 1227–1249.

Granjeon, D., Joseph, P., 1999. Concepts and applications of a 3D multiple lithology, diffusive model in stratigraphic modelling. In: Harbaugh, J.W., et al. (Ed.), Numerical Experiments in Stratigraphy. SEPM Special Publications, vol. 62, pp. 197–210.

Groshong, R.H., 1972. Strain calculated from twinning in calcite. Geological Society of America Bulletin 83, 2025–2048.

Halley, R.B., Pierson, B.J., Schlager, W., 1984. Alternative diagenetic models for Cretaceous talus deposits, DSDP Site 536, Gulf of Mexico. In: Buffler, R.T., Schlager, W. (Eds.), Init. Repts. DSDP, vol. 11. U.S. Govt. Printing Office, Washington, pp. 397–408.

Harris, J.H., Van der Pluijm, B.A., 1998. Relative timing of calcite twinning strain and fold–thrust belt development: Hudson Valley fold–thrust belt, New York, USA. Journal of Structural Geology 20, 21–31.

Hendry, J.P., Trewin, N.H., Fallick, A.E., 1996. Low-Mg calcite marine cement in Cretaceous turbidites: origin, spatial distribution and relationship to seawater chemistry. Sedimentology 43 (5), 877–900.

Holl, J.E., Anastasio, D.J., 1995. Cleavage development within a foreland fold and thrust belt, southern Pyrenees, Spain. Journal of Structural Geology 17, 357–369.

Hung, J.-H., Kuo, C.-K., 1999. Calcite twins for determining paleostrain and paleostress in the thrust front of the Taiwan collisional belt. Journal of the Geological Society of China 42, 209–232.

Jamison, W.R., Spang, J., 1976. Use of calcite twin lamellae to infer differential stresses. Geological Society of America Bulletin 87, 868–887.

Kiratzi, A., Muço, B., 2004. Seismotectonics and seismic hazard assessment in Albania. NATO Science for Peace Programme. final report.

Kodra, A., Bushati, S., 1991. Paleotectonic emplacement of the ophiolites of Mirdita zone. Buletini i Shkencave Gjeologjike 1, 99–108 (in Albanian).

Lacombe, O., 2001. Paleostress magnitudes associated with development of mountain belts: Insights from tectonic analyses of calcite twins in the Taiwan Foothills. Tectonics, 20 6, 834–849.

Lacombe, O., 2007. Comparison of paleostress magnitudes from calcite twins with contemporary stress magnitudes and frictional sliding criteria in the continental crust: Mechanical implications. Journal of Structural Geology 29, 86–99.

Lacombe, O., Laurent, P., 1996. Determination of deviatoric stress tensors based on inversion of calcite twin data from experimentally deformed monophase samples: preliminary results. Tectonophysics 255, 189–202.

Lacombe, O., Angelier, J., Laurent, P., Bergerat, F., Tourneret, C., 1990. Joint analyses of calcite twins and fault slips as a key for deciphering polyphase tectonics: burgundy as a case study. Tectonophysics 182, 279–300.

Lacombe, O., Angelier, J., Laurent, P., 1993. Les macles de la calcite, marqueurs des compressions récentes dans un orogène actif: l'exemple des calcaires récifaux du sud de Taiwan. Comptes Rendus de l'Académie Sciences, Sereis II 316, 1805–1813.

Lacombe, O., Amrouch, K., Mouthereau, F., Dissez, L., 2007. Calcite twinning constraints on late Neogene stress patterns and deformation mechanisms in the active Zagros collision belt. Geology 35 (3), 263–266. doi:10.1130/G23173A.1.

Laurent, P., Kern, H., Lacombe, O., 2000. Determination of deviatoric stress tensors based on inversion of calcite twin data from experimentally deformed monophase samples, part II, Uniaxial and triaxial stress experiments. Tectonophysics 327, 131–148.

Lohmann, K.C., 1988. Geochemical patterns of meteoric diagenetic systems and their application to studies of paleokarst. In: James, N.P., Choquette, P.W. (Eds.), Paleokarst. Springer-Verlag, New-York, pp. 58–80.

Mantovani, E., Albarello, D., Babbucci, D., Tamburelli, C., Viti, M., 2002. Trench arc-back arc systems in the Mediterranean area: examples of extrusion tectonics. 2002 In: Rosenbaum, G., Lister, G.S. (Eds.), Reconstruction of the Evolution of the Alpine–Himalayan Orogeny. Journal of the Virtual Explorer.

Marfil, R., Caja, M.A., Tsige, M., Al-Aasm, I.S., Martin-Crespo, T., Salas, R., 2005. Carbonate-cemented stylolites and fractures in the Upper Jurassic limestones of the Eastern Iberian Range, Spain: a record of palaeofluids composition and thermal history. Sedimentary Geology 178, 237–257.

Mattavelli, L., Novelli, L., Anelli, L., 1991. Occurrence of hydrocarbons in the Adriatic basin. In: Spencer, A.M. (Ed.), Generation, Accumulation and Production of Europe's Hydrocarbons. European Assoc. Petrol. Geosc., Spec. Publ., vol. 1. Springer, Oxford, pp. 369–380.

McArthur, J.M., Howarth, R.J., 2004. Sr-isotope stratigraphy: the Phanerozoic $^{87}Sr/^{86}Sr$—curve and explanatory notes. In: Gradstein, F., Ogg, J., Smith, A.G. (Eds.), A Geological Timescale, vol. 7. CUP. 589 pp.

Meço, S., Aliaj, S., 2000. Geology of Albania. Beiträge zur Regionalen Geologie der Erde. Gebrüder Borntraeger, Berlin. 246 pp.

Melo, V., Shallo, M., Aliaj, Sh., Xhomo, A., Bakia, H., 1991a. Thrust and nappe tectonics in geological structure of Albanides. Buletini i Shkencave Gjeologjike 1, 7–20 (in Albanian).

Melo, V., Aliaj, S.h., Kora, A., Xhomo, P., Naso, F., Lula, K., Gjata, V., Hoxhe, V., 1991b. Tectonic windows of the external zones in the eastern regions of Albanides. Buletini i Shkencave Gjeologjike 1, 21–29 (in Albanian).

Monopolis, D., Bruneton, A., 1982. Ionian sea (western Greece): its structural outline deduced from drilling and geophysical data. Tectonophysics 83, 227–242.

Moretti, I., Larrère, M., 1989. LOCACE: computer-aided construction of balanced geological cross-section. Geobyte 4, 1–24.

Moretti, I., Colletta, B., Vially, R., 1988. Theoretical model of block rotation along circular faults. Tectonophysics 153, 313–320.

Muceku, B., 2006. Evolution verticale des Albanides: contrôle thermique, érosion et dénudation tectonique. PhD thesis, 279 pp.

Muceku, B., Mascle, G.H., Tashko, A., 2006. First results of fission-track thermochronology in the Albanides. Geol. Society of London, Spec. Publ., vol. 260, pp. 539–556.

Muska, K., 2002. Thermicité, transferts et diagenèse des réservoirs dans les unités externes des Albanides (Bassin Ionien). PhD Thesis, UPMC Paris VI, IFP Report 56850, 205 pp.

Nielsen, P., Swennen, R., Keppens, E., 1994. Multiple-step recrystallization within massive ancient dolomite units: an example from the Dinantian of Belgium. Sedimentology 41, 467–584.

Nieuwland, D.A., Oudmayer, B.C., Valbona, U., 2001. The tectonic development of Albania: explanation and prediction of stuctural styles. Marine and Petroleum Geology 18, 161–177.

Ramsay, J.G., 1980. The Crack-seal mechanism of rock deformation. Nature 284, 135–139.

Rigakis, N., Karakitsios, V., 1998. The source rock horizons of the Ionian basin (NW Greece). Marine and Petroleum Geology 15, 593–617.

Robertson, A., Shallo, M., 2000. Mesozoic–Tertiary tectonic evolution of Albania in its regional eastern Mediterranean context. Tectonophysics 316, 197–254.

Rocher, M., Lacombe, O., Angelier, J., Chen, H.W., 1996. Mechanical twin sets in calcite as markers of recent collisional events in a fold-and-thrust belt: evidence from the reefal limestones of southwestern Taiwan. Tectonics 15 (5), 984–996.

Rocher, M., Lacombe, O., Angelier, J., Deffontaines, B., Verdier, F., 2000. Cenozoic folding and faulting in the North Pyrenean Foreland (Aquitaine Basin, France): insights from combined structural and paleostress analyses. Journal of Structural Geology 22 (5), 627–645.

Roure, F., Prenjasi, A., Xhafa, Z., 1995. Petroleum geology of the Albanian foothills. AAPG Nice, Post-Conference Guide-Book. 100 pp.

Roure, F., Nazaj, S., Muska, K., Fili, I., Cadet, J.P., and Bonneau, M., 2004. Kinematic evolution and petroleum systems: an appraisal of the Outer Albanides. In: McKlay, ed., Thrust Tectonics and Hydrocarbon Systems, AAPG Mem. 82, 24, 474–493.

Roure, F., Swennen, R., Schneider, F., Faure, J.L., Ferket, H., Guilhaumou, N., Osadetz, K., Robion, Ph., Vandeginste, V., 2005. Incidence and importance of Tectonics and natural fluid migration on reservoir evolution in foreland fold-and-thrust belts. In: Brosse, E., et al. (Ed.), Oil and Gas Science and Technology, Oil and Gas Science and Technology, Revue de l'IFP, vol. 60, pp. 67–106.

Rowe, K.J., Rutter, E.H., 1990. Paleostress estimation using calcite twinning: experimental calibration and application to nature. Journal of Structural Geology 12 (1), 1–17.

Sassi, W., Rudkiewicz, J.L., 1999. THRUSTPACK version 6.2: 2D Integrated Maturity Studies in Thrust Areas. IFP internal report n° 45372, 79 pp.

Sassi, W., Graham, R., Gillcrist, R., Adams, M., Gomez, R., 2007. The impact of deformation timing on the prospectivity of the Middle Magdalena sub-thrust, Colombia. Geological Society, London, Special Publications, vol. 272, pp. 473–498.

Schneider, F., 2003. Basin modelling in complex area: examples from eastern Venezuela and Canadian foothills. Oil and Gas Science and Technology, Revue de l'IFP 58 (2), 313–324.

Schneider, F., Devoitine, H., Faille, I., Flauraud, E., Willien, F., 2002. Ceres 2D: a numerical prototype for HC potential evaluation in complex area. Oil and Gas Science and Technology, Revue de l'IFP 54 (6), 607–619.

Shallo, M., 1991. Albanian ophiolites. Sci. Rep., Tirana, Albania. 247 pp. (in Albanian).

Shallo, M., 1992. Geological evolution of the Albanian ophiolite and their platform periphery. Geologische Rundschau 81, 681–694.

Speranza, F., Islami, I., Kissel, C., Hyseni, A., 1995. Paleomagnetic evidence for Cenozoic clockwise rotation of the external Albanides. Earth and Planetary Science Letters 129, 121–134.

Suppe, J., 1983. Geometry and kinematics of fault-bend folding. American Journal of Science 283, 684–721.

Swennen, R., Van Geet, M., Roure, F., Müller, C., Nazaj, S., Mushka, K., Zaimi, L., 1999. Subtrap Albanian transect across the Ionian Basin and Kremenara anticline. IFP-SUBTrap report, n° 45635-1.

Swennen, R., Muska, K., Roure, F., 2000. Fluid circulation in the Ionian fold and thrust belt (Albania): implications for hydrocarbon prospectivity. Journal of Geochemical Exploration 69, 629–634.

Tagari, D., 1993. Etude néotectonique et sismotectonique des Albanides: analyse des déformations et géodynamique du Langhien à l'Actuel. PhD Thesis, Paris XI, Orsay.

Townend, J., Zoback, M.D., 2000. How faulting keeps the crust strong. Geology 28 (5), 399–402.

Tozer, R.S.J., Butler, R.W.H., Chiappini, M., Corrado, S., Mazzoli, S., Speranza, F., 2006. Testing thrust tectonic models at mountain fronts: where has the displacement gone? Journal of the Geological Society, London 163, 1–14.

Travé, A., Calvet, F., Sans, M., Verges, J., Thirlwall, M., 2000. Fluid history related to the Alpine compression at the margin of the South Pyrenean Foreland Basin; the El Guix Anticline. Tectonophysics 321 (1), 73–102.

Turner, F.J., Griggs, D.T., Heard, H.C., 1954. Experimental deformation of calcite crystals. Geological Society of America Bulletin 65, 883–934.

Underhill, J., 1988. Triassic evaporites and Plio-Quaternary diapirism in western Greece. Journal of the Geological Society of London 145, 269–282.

Van Geet, M., Swennen, R., Durmishi, C., Roure, F., Muchez, P., 2002. Paragenesis of Cretaceous to Eocene carbonate reservoirs in the Ionian foreland fold-and-thrust belt (Albania): relation between tectonism and fluid flow. Sedimentology 49, 697–718.

Vandeginste, V., Swennen, R., Ellam, R., Schneider, F., 2005. Zebra dolomitization as a result of focussed fluid flow during fold-and-thrust belt development (Middle Cambrian, Canadian Rocky Mountain). Sedimentology 52, 1067–1095.

Vandeginste, V., Swennen, R., Gleeson, S.A., Ellam, R., Osadetz, K., Roure, F., 2006. Development of secondary porosity in the Fairholme carbonate complex (south-west Alberta, Canada). Journal of Geochemical Exploration 89 (1–3), 394–397.

Velaj, T., 2001. Evaporites in Albania and their impact on the thrusting processes. Journal of the Balkan Geophysical Society 4 (1), 9–18.

Velaj, T., Xhufi, C., 1995. The evaporite effect on the tectonic style of the internal Ionian subzone of the Albanides. The 57th EAGE Conference and Technical exhibition, Glasgow, Abst., p. 574.

Velaj, T., Davison, I., Serjani, A., Alsop, I., 1999. Thrust tectonics and the role of evaporites in the Ionian Zone of the Albanides. AAPG Bulletin 83 (9), 1408–1425.

Vilasi, N., Swennen, R., Roure, F., 2006. Diagenesis and fracturing of Paleocene–Eocene carbonate turbidite systems in the Ionian Basin: the example of the Kelcyra area (Albania). Journal of Geochemical Exploration 89, 409–413.

Zappatera, E., 1994. Source rock distribution model of the Periadriatic region. AAPG Bulletin 78/3, 333–354.